

# UC San Diego

## UC San Diego Electronic Theses and Dissertations

### Title

Targeting atherosclerosis : nanoparticle delivery for diagnosis and treatment

### Permalink

<https://escholarship.org/uc/item/0wk9q0d5>

### Author

Peters, David Thomas

### Publication Date

2009

Peer reviewed|Thesis/dissertation

UNIVERSITY OF CALIFORNIA, SAN DIEGO

Targeting Atherosclerosis: Nanoparticle Delivery for Diagnosis and Treatment

A dissertation submitted in partial satisfaction of the  
requirements for the degree Doctor of Philosophy

in

Biomedical Sciences

by

David Thomas Peters

Committee in Charge:

Professor Stephen Howell, Chair  
Professor Erkki Ruoslahti, Co-Chair  
Professor Jeffrey Esko  
Professor James Feramisco  
Professor Richard Lieber

2009

Copyright

David Thomas Peters, 2009

All rights reserved.

The Dissertation of David Thomas Peters is approved, and it is acceptable in quality and form for publication on microfilm and electronically:

---

---

---

---

Co-Chair

---

Chair

University of California, San Diego

2009



## DEDICATION

I would like to dedicate my dissertation to my wife, Tiffany Peters, without whose love and support I could not have made it through this graduate program.

I would also like to dedicate this to the rest of my family, especially my mother who convinced me to continue on with school but unfortunately didn't get to see me finish.

## TABLE OF CONTENTS

Signature Page.....	iii
Dedication.....	iv
Table of Contents.....	v
List of Figures.....	vii
Acknowledgements.....	x
Vita.....	xi
Abstract of the Dissertation.....	xiii
Chapter 1     Introduction	
History and Morbidity.....	1
Pathogenesis of Atherosclerosis.....	3
Diagnosis and Treatments.....	6
Targeted therapies for atherosclerosis.....	10
References.....	12
Chapter 2     Animal models of Atherosclerosis	
Abstract.....	17
Introduction.....	17
Methods.....	21
Results.....	24
Discussion.....	28
References.....	31

Chapter 3	Discovering new atherosclerotic plaque targeting ligands using <i>in vivo</i> phage display	
	Abstract.....	34
	Introduction.....	34
	Methods.....	38
	Results.....	41
	Discussion.....	46
	References.....	48
Chapter 4	Targeting atherosclerosis using CREKA targeted, modular, multifunctional micelles	
	Abstract.....	50
	Introduction.....	50
	Methods.....	53
	Results.....	58
	Discussion.....	68
	References.....	71
Chapter 5	Conclusion.....	74

## LIST OF FIGURES

Figure 1.1: Narrowing of blood vessel due to atherosclerotic plaque. The plaque that forms in the vessel wall protrudes into the lumen of the vessel and narrows the opening compared to the healthy vessel. This decrease in the diameter of the lumen causes a disruption in blood flow.....	2
Figure 1.2: Pathogenesis of Atherosclerosis. Turbulence and risk factors injure the endothelial cells (EC) in the blood vessel. This allows inflammatory cells to bind and extravasate into the vessel wall. Low-density lipoproteins move in and out of the vessel wall some of which attach to.....	5
Figure 1.3: Differences between stable and vulnerable plaques. Plaques that are vulnerable to rupture generally have a large lipid core (seen in yellow), fewer smooth muscle cells, and lots of inflammation. On the other hand, stable plaques that are resistant to rupture are more fibrous.....	6
Figure 2.1: Effect of R-Ras on smooth muscle cell attachment and intimal hyperplasia. (A) Cultured smooth muscle cells exhibit more attachment and spreading when transfected with a constitutively active form of R-Ras (R-Ras38V). (B) Increased intimal hyperplasia.....	20
Figure 2.2: ApoE null mouse model of atherosclerosis. (A) Wild-type (left, 20g) and ApoE null mouse fed high fat diet for 16 weeks (right, 48g). (B) Total blood cholesterol in wild-type, ApoE null, and ApoE null mouse on a high fat diet (Error bars represent standard error.....	24
Figure 2.3: Morphology of plaques in ApoE null mice. Tissue cross-sections (5µm thick) of the brachiocephalic artery were cut with from wildtype (A) and ApoE null mice fed a high fat diet for 6 months (B, C). Nuclei are stained with DAPI in blue. (C) Buried fibrous caps were.....	25
Figure 2.4: ApoE/SRBI double knockout model of atherosclerosis. Mice null for both the ApoE and SRBI proteins developed fatty streaks in their aorta and thromboses in their coronary arteries in as little as 5 weeks after birth on a standard chow diet, and died of myocardial .....	27
Figure 2.5: Genotyping ApoE/SRBI/R-Ras triple knockout mice. Genomic DNA was isolated from tail clips of mice. Separate PCR reactions were performed to determine the genotype for each gene and the PCR products were run on a 2% agarose gel.....	28

Figure 2.6: Survival curve of ApoE null (sKO), ApoE/SRBI null (dKO), and ApoE/SRBI/R-Ras null (tKO) mice. sKO mice on a high fat diet do not have a decreased life span. tKO mice had a significantly longer lifespan than dKO mice, 49 and 43 days, respectively ( $p \leq 0.05$ , $n=17$ .....	28
Figure 3.1: <i>In vivo</i> phage display using T7 phage library. (A) Structure of T7 phage. T7 is an icosahedral phage made up of 415 capsid proteins arranged in 60 hexamers at the faces and 11 pentamers at the vertices making up the capsid. Attached to the capsid is a head-tail connector.....	36
Figure 3.2: PCR mutagenesis of T7 phage vector. Mutagenesis was performed in two steps. In the first reaction the mutations were introduced into the DNA sequence and the ApaLI-up and right V/D primers produced a 1204bp product and the left V/D and .....	39
Figure 3.3: Mutations in the tail protein of long-circulating T7 phage. Two mutations were made in gene 17 of the phage, disrupting the coiled-coil structure of the tail proteins. The strong positive charge of the arginine residue at position 207 was converted to a neutral charge.....	42
Figure 3.4: Effect of tail mutations on T7 phage circulation time. T7 phage with two amino acid substitutions in the tail fiber protein have a much longer circulation time in the blood of mice than wild-type T7 phage ( $n=6$ mice for R207V/K211D mutant phage and $n=3$ mice.....	43
Figure 3.5: Phage playoff screen of known homing peptides for atherosclerotic plaques. Various phage clones expressing peptides that are known to target tumor blood vessels were pooled together and injected into an atherosclerotic, ApoE null mouse on a high fat diet. The aortic.....	44
Figure 3.6: Phage homing to atherosclerotic plaques. Individual phage clones expressing various peptides that are known to target tumor blood vessels were individually injected into ApoE null mice on a high fat diet. The aortic tree containing atherosclerotic plaques and vessels that did.....	45
Figure 4.1: Structure and homing of carboxyfluorescein (FAM)-CREKA penta-peptide. (A) Chemical structure of FAM-CREKA. (B) FAM-CREKA bound to the blood vessels and stroma of B16F1 melanoma tumors in wild-type mice but not mice that lack fibrinogen.....	52

Figure 4.2: Thrombin activity chromogenic assay. Excess thrombin was incubated with the sample containing hirudin and allowed to complex. Residual thrombin cleaves the chromogenic substrate S-2366 into a peptide and free p-nitroaniline (pNA) which absorbs light at 405nm.....	55
Figure 4.3: Construction of modular, multifunctional micelles. (A) Individual lipopeptide monomers are made up of a 1,2-distearoyl-sn-glycero-3-phosphoethanol-amine (DSPE) tail, a polyethyleneglycol (PEG2000) spacer, and a variable polar headgroup that contains either .....	59
Figure 4.4: <i>Ex vivo</i> imaging of the aortic tree of atherosclerotic mice. Micelles were injected intravenously and allowed to circulate for three hours. The aortic tree was excised following perfusion and imaged <i>ex vivo</i> . (A) Increased fluorescence was observed in the aortic tree of.....	61
Figure 4.5: Binding of FAM-CREKA micelles to atherosclerotic plaque. ApoE null mice were injected with FAM-CREKA micelles which were allowed to circulate for 3 hours. Mice were perfused to remove unbound micelles and tissue cross-sections of the .....	62
Figure 4.6: Localization of CREKA micelles in atherosclerotic plaques. (A) Serial cross-sections (5µm thick) were stained with antibodies against CD31 (endothelial cells), CD68 (macrophages and other lymphocytes), and fibrinogen. Representative.....	63
Figure 4.7: Targeting micelles to atherosclerotic plaques. ApoE null and wild-type mice were injected intravenously with FAM-CREKA micelles, which were allowed to circulate for 3 hours. (A, C) The aortic tree was excised following perfusion and imaged.....	64
Figure 4.8: Role of clotting in binding of CREKA micelles. (A) Mice were injected intravenously with PBS or a bolus of 800 units/kg of heparin, followed 60 minutes later by 100µl of 1mM FAM-CREKA micelles. The mice received additional heparin (a total of 1,000.....	65
Figure 4.9: Targeting of hirulog to atherosclerotic plaques. (A) Equal molar concentrations of hirulog peptide and hirulog micelles were tested for anti-thrombin activity to ensure that potency did not decrease when hirulog was in micellar form. Hirulog peptide and micelles showed.....	66
Figure 4.10: CREKA micelle homing after hirulog anticoagulant therapy. ApoE knockout mice on a high fat diet for 6 months were injected intravenously every 12 hours with 100µl, 1mM hirulog micelles for 72 hours. Either non-targeted or CREKA targeted micelles injected.....	68

## ACKNOWLEDGEMENTS

I would like to acknowledge Professor Erkki Ruoslahti for his support as my mentor and advisor during my graduate studies. I would also like to acknowledge everyone in the Ruoslahti lab, whose help with setting up experiments and learning techniques was invaluable and without whom my research would have taken considerably longer.

In Chapter 2 the ApoE/SR-BI double knockout mice were a gift from Dr. Monty Krieger at MIT.

Chapter 4, in part, has been submitted for publication of the material as it may appear in *Proceedings of the National Academy of Sciences*, 2009, Targeting atherosclerosis using modular, multifunctional micelles. David Peters, Mark Kastantin, Ramana Kotamraju, Priya P. Karmali, Kunal Gujraty, Matthew Tirrell, and Erkki Ruoslahti. The dissertation author was the primary investigator and author of this paper. We also thank Dr. Lilach Agemy for the 22RV1 mouse prostate tumor model and Peter Allen for the micelle graphic.

## VITA

- 2000 Bachelor of Science in Animal Physiology and Neuroscience, University of California, San Diego
- 2000 Bachelor of Science in Psychology, University of California, San Diego
- 1999-2003 Research Assistant in Muscle Physiology and Orthopedics Lab, University of California, San Diego
- 2002 Master of Science in Biology, University of California, San Diego
- 2000-2003 Teaching Assistant in Physiology, University of California, San Diego
- 2004-2009 Research Assistant in Vascular Mapping Center, Burnham Institute for Medical Research
- 2009 Doctor of Philosophy in Biomedical Sciences, University of California, San Diego

## PUBLICATIONS

**Peters, D.**, Kastantin, M., Kotamraju, R., Gujraty, K., Tirrell, M., Ruoslahti, E. (2008) Targeting atherosclerosis using modular, multifunctional micelles. *PNAS*, (Submitted).

Pilch, J., Brown, D. M., Komatsu, M., Jarvinen, T. A., Yang, M., **Peters, D.**, Hoffman, R. M., Ruoslahti, E. (2006) Peptides selected for binding to clotted plasma accumulate in tumor stroma and wounds. *PNAS*, 103: 2800-2804.

Hentzen, E. R., Lahey, M., **Peters, D.**, Mathew, L., Barash, I. A., Friden, J., Lieber, R. L. (2006) Stress-dependent and stress-independent expression of the myogenic regulatory factors and the MARP genes after eccentric contractions. *J. Physiol. (London)*, 570:157-67.

Akerman, M.E., Pilch, J., **Peters, D.**, Ruoslahti, E. (2005) Angiostatic peptides use plasma fibronectin to home to angiogenic vasculature. *PNAS*, 102:2040-2045.

**Peters, D.**, Burdi, M., Barash, I., Yuan, P., Friden, J., Lutz, G., Lieber, R. L. (2003) Asynchronous Functional, Cellular, and Transcriptional Changes After a Bout of Eccentric Exercise in the Rat. *J. Physiol. (London)*, 553:947-957.



Barash, I. A., **Peters, D.**, Friden, J., Lutz, G. J., Lieber, R. L. (2002) Desmin Cytoskeletal Desmin cytoskeletal modifications after a bout of eccentric exercise in the rat. *Am J Physiol Regul Integr Comp Physiol*, Oct; 283(4):R958-63.

Shah S. B., **Peters D.**, Jordan K. A., Milner D. J., Friden J., Capetanaki Y., Lieber R. L. (2001) Sarcomere number regulation maintained after immobilization in desmin-null mouse skeletal muscle. *J Exp Biol*, May; 204(Pt 10):1703-10.

## ABSTRACT OF THE DISSERTATION

Targeting Atherosclerosis: Nanoparticle Delivery for Diagnosis and Treatment

by

David Thomas Peters

Doctor of Philosophy in Biomedical Sciences

University of California, San Diego, 2009

Professor Stephen Howell, Chair  
Professor Erkki Ruoslahti, Co-Chair

Atherosclerosis is a type of arteriosclerosis, or hardening of the blood vessels that is due to the deposition of plaques in the vessel wall. Recently, it has become clear that not all plaques are the same and that those with large lipid, necrotic cores and thin fibrous caps can rupture and lead to acute events such as myocardial infarction, stroke, and death. Atherosclerosis is a complex disease that takes years to develop in humans and has been difficult to duplicate in an animal model. Two animal models of atherosclerosis were studied to determine if they could be used to identify novel targeting peptides for lesions that were vulnerable to rupture and a new animal model was developed to study the stabilization of vulnerable plaques.

Phage display using T7 bacteriophage is a powerful technique both *in vitro* and *in vivo* to find peptides that specifically bind to various proteins and surfaces. The T7

phage vector was optimized to increase the circulation time of the phage by introducing two mutations into the tail proteins of the phage that decreased their uptake by the liver. Phage display was then used to test various peptides which bind to tumor vasculature *in vivo* to determine if they also bind to atherosclerotic plaques.

One such peptide, CREKA, binds to clotted plasma proteins and was used to target atherosclerotic plaques in ApoE null mice fed a high fat diet. Subtle clotting that occurs on the luminal surface of atherosclerotic plaques, presents a novel target for nanoparticle-based diagnostics and therapeutics. We have developed multifunctional, modular micelles that contain a targeting element, a fluorophore and, when desired, a drug component in the same particle. The fluorescent micelles bind to the entire surface of the plaque and notably, concentrate at the shoulders of the plaque, a location that is prone to rupture. We also show that the targeted micelles deliver an increased concentration of the anticoagulant drug, hirulog, to the plaque when compared to untargeted micelles.

## Chapter 1

### **Introduction**

#### **History and Morbidity**

Atherosclerosis is a type of arteriosclerosis, or hardening of the blood vessels, that is due to an atheromatous plaque formation in the vessel wall. Félix J. Marchand is credited with coining the term in the 1860s. The term is derived from the Greek word “athero” which means porridge or gruel, and describes the soft, lipid rich inflammatory material seen in most atherosclerotic lesions and “sclerosis” which means scarring or hardening. It is a condition that results in a narrowing or obstruction of the blood vessels leading to strokes, heart attacks, and death (Fig 1.1). Cardiovascular disease, which atherosclerosis is a major cause of, affects 1 in 3 American adults and costs over \$400 billion in direct and indirect expenses using 8% of overall healthcare spending each year (Rosamond, Flegal et al. 2007). Environmental as well as genetic risk factors for the disease have been determined, including; a family history of the disease, high levels of low density lipoprotein (LDL) in the blood, high blood pressure, smoking, gender, race, diabetes, excess weight, a high fat diet, high alcohol intake, and a sedentary lifestyle. All of these risk factors contribute to the likelihood of developing the disease. Atherosclerosis is an insidious disease though, and takes years to develop before any symptoms begin to show.

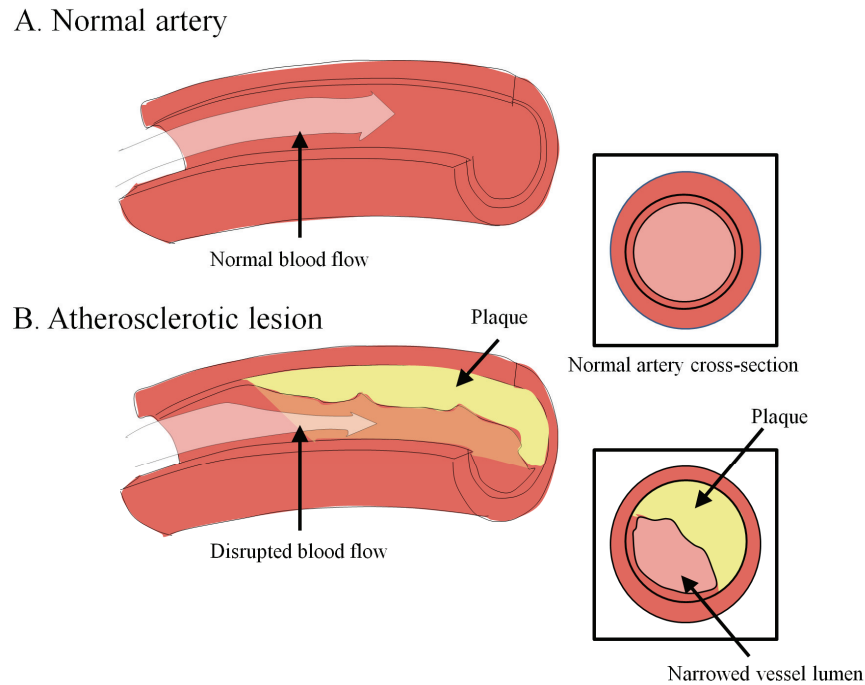


**Figure 1.1:** Narrowing of blood vessel due to atherosclerotic plaque. The plaque that forms in the vessel wall protrudes into the lumen of the vessel and narrows the opening compared to the healthy vessel. This decrease in the diameter of the lumen causes a disruption in blood flow.

Atherosclerosis has affected humans for thousands of years. Microscopic and macroscopic evidence of vascular lesions have been found in the aorta and also carotid, coronary, and femoral arteries of Egyptian mummies (Ruffer 1911; Ruffer 1920). The implications of vascular lesions were first described by James B. Herrick, an American physician in 1912 when he published a paper in the *Journal of the American Medical Association* describing the clinical features of myocardial infarction (Herrick 1983). Prior to the 20<sup>th</sup> century, atherosclerosis was a rare disease that affected few individuals, but in less than 100 years it has grown into the number one killer in the United States. Technology and innovation have made life less strenuous and more sedentary. Manual labor has been replaced or assisted by machinery. Automobiles, washing machines, elevators, and vacuum cleaners have all become commonplace. A change in diet has

accompanied the lifestyle change and high fat foods, including butter, cheese, ice cream, hamburgers, fries, and potato chips have become a staple of the western diet. The average lifespan has also increased about 30 years in the last century, from 44-45 years for males and 49-50 years for females in 1900 to 74-75 years for males and 79-80 years for females in 1999 (CDC 1999). All of these changes in the life of an average American have contributed to the growth of atherosclerosis.

### **Pathogenesis of Atherosclerosis**

The process of atherosclerosis begins in infancy with the development of fatty streaks in the vessels (Napoli, D'Armiento et al. 1997). The fatty streak is made up almost entirely of monocyte derived macrophages and T-lymphocytes (Stary, Chandler et al. 1994). The number of fatty streaks increases with age throughout adolescence and early adulthood. More advanced lesions begin to develop in the mid 20's and progress with age. Clinical manifestations of the disease begin to appear with the advent of advanced plaques and the frequency also increases with age through the 50's and 60's.

It is now widely accepted that atherosclerosis is a chronic inflammatory disease (Blake and Ridker 2002; Buffon, Biasucci et al. 2002; George 2008; Lamon and Hajjar 2008). Insults to the endothelial layer in areas of turbulent blood flow in the vasculature, such as branch points, lead to overexpression of vascular cell adhesion molecule 1 (VCAM-1) in the endothelial cells (Cybulsky and Gimbrone 1991). VCAM-1 expression is very important in the initiation of atherosclerosis and lesions are

reduced in mice lacking VCAM-1 (Li and Glass 2002). Its expression leads to recruitment of T-cells and monocytes to the site of endothelial injury. Recruited leukocytes then amplify the inflammatory reaction by releasing monocyte chemo-attractant protein-1 (MCP-1) which recruits additional leukocytes, activates leukocytes in the media, and causes recruitment and proliferation of smooth muscle cells (Yla-Herttuala, Lipton et al. 1991). Recruited macrophages also release more cytokines and extravasate into the medial layer of the vessel. Local activation of monocytes leads to both cytokine-mediated progression of atherosclerosis, and oxidation of low-density lipoprotein. Lowering levels of chronic inflammation is a major target of atherosclerotic research. Many of the beneficial effects of “statins” also appear to be mediated through their ability to modify the inflammatory cascade (Palinski and Tsimikas 2002; Schonbeck and Libby 2004).

Cholesterol moves in and out of the vessel wall attached to transport proteins in the form of LDL. When LDL is present in the subintimal space it can either cross back out into the bloodstream unchanged or it can become oxidized by oxygen free radicals in the presence of inflammation and become trapped. Lipoxygenases (LOs), myeloperoxidase (MPO), inducible nitric oxide synthase (iNOS) and NADPH oxidases are all thought to contribute to the oxidation of LDL and are expressed by macrophages (Malle, Marsche et al. 2006). Oxidized LDL (oxLDL) binds to scavenger receptors on the surface of macrophages and is taken up into the cell (Matsuura, Kobayashi et al. 2006). Macrophages take up massive amounts of oxLDL and store the excess cholesterol as cholesterol ester droplets transforming the cells into foam cells. Uptake

of the oxLDL makes the foam cells less mobile, promoting the accumulation of lipid laden cells in the intima. Foam cells secrete additional cytokines which attract more monocytes and cause smooth muscle cells to proliferate (Fig 1.2). The plaque gradually enlarges over time due to accumulation of foam cells and smooth muscle cells in the intima .

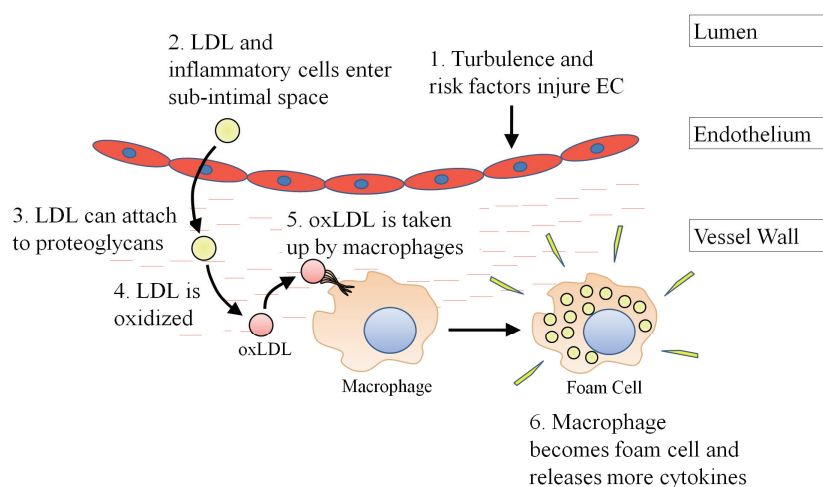


**Figure 1.2:** Pathogenesis of Atherosclerosis. Turbulence and risk factors injure the endothelial cells (EC) in the blood vessel. This allows inflammatory cells to bind and extravasate into the vessel wall. Low-density lipoproteins move in and out of the vessel wall some of which attach to proteoglycans in the subintimal space. LDL that is attached to proteoglycans is oxidized and then recognized by scavenger receptors on macrophages. Lipid laden macrophages become foam cells and are trapped in the vessel wall. Foam cells release cytokines that attract more monocytes to the area and cause smooth muscle cells in the blood vessel to proliferate.

Depending on the plaque's morphology it can become a stable, fibrous plaque or a plaque that is vulnerable to rupture (Loftus and Thompson 2008). Stable plaques can lead to chronic complications such as angina as they grow and cause the lumen of the vessel to narrow, but they are generally considered to cause a benign disease. On the other hand, asymptomatic, unstable plaques can rupture, exposing their contents to the bloodstream and initiate the coagulation cascade. This produces a thrombus on the



surface of the plaque and can either occlude the vessel at the plaque or break off and lodge into smaller blood vessels downstream, causing a myocardial infarction or stroke. Those plaques that are at a higher risk for rupture generally exhibit large lipid cores, thin fibrous caps, lots of inflammatory cells, especially macrophages, lipid peroxidases, and fewer vascular smooth muscle cells (Figure 1.3, Libby 2001; Fuster, Fayad et al. 2005; Fuster, Moreno et al. 2005).

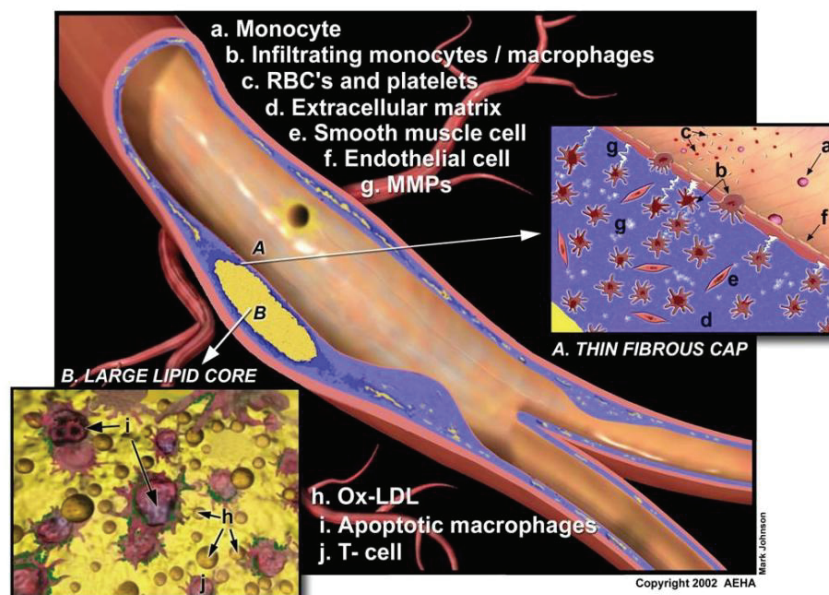


**Figure 1.3:** Differences between stable and vulnerable plaques. Plaques that are vulnerable to rupture generally have a large lipid core (seen in yellow), fewer smooth muscle cells, and lots of inflammation. On the other hand, stable plaques that are resistant to rupture are more fibrous and contain a higher number of smooth muscle cells compared to unstable plaques.

## Diagnosis and Treatments

Atherosclerosis is generally not diagnosed until after complications occur, such as loss of sensation in the extremities, chest pain, myocardial infarction, or death from decreased blood flow to the tissues. Currently, the degree and location of the blockage is determined using contrast-enhanced X-ray angiography in which a dye is injected

into the bloodstream and blood flow is imaged. Areas where blood flow is restricted due to a plaque will have an absence of dye. This technique remains the gold standard for evaluation of cardiovascular disease. This imaging technique is limited in that it cannot quantify the extent of plaque coverage in the vasculature and is only a measure of disrupted blood flow. Angiograms also do not provide information about the morphology or stability of the plaque. Plaque vulnerability does not appear to be dependent on plaque size (Carr, Farb et al. 1996; Virmani, Kolodgie et al. 2000; Virmani, Burke et al. 2003). Therefore, small, asymptomatic plaques that are vulnerable to rupture may be missed by conventional X-ray angiography. Newer technology using computed tomography (CT) or magnetic resonance imaging (MRI) is now available to perform angiography, giving pictures with more detail, but angiograms are still limited in the information that they provide. Targeted imaging techniques which can deliver contrast or radiotracer agents directly to the atherosclerotic plaque by targeting specific components or cell surface markers in the lesion are becoming closer to a reality in the clinic. These techniques would allow high resolution imaging such as MRI or PET to be used to non-invasively image individual plaques.

Current treatments for atherosclerosis try to alleviate the symptoms of the disease or slow its progression. Cholesterol lowering drugs such as 3-hydroxy-3-methylglutaryl coenzyme A (HMG-CoA) reductase inhibitors, or “statins”, are used to decrease cholesterol synthesis and increase clearance of LDL through the liver causing a general decrease in blood cholesterol. Use of statins have translated into a 60% decrease in myocardial infarctions and a 17% drop in strokes (Law, Wald et al. 2003),

but they have not turned out to be the cure-all that was hoped for when they were discovered (Amarenco and Tonkin 2004) and have their own side effects.

Anticoagulants such as heparin, warfarin, low dose aspirin, and the direct thrombin inhibitors, are used to prevent a thrombus from forming if a plaque ruptures. These drugs are given systemically and have many potential side effects such as severe hemorrhage, thrombocytopenia, and drug interactions. Heparin, one of the most widely used anticoagulants in the hospital, also has a variable effect in patients. This may be due to the fact that it binds to many plasma proteins such as fibronectin, vitronectin, and von Willebrand factor and is also neutralized by platelet factor 4 and histidine-rich glycoproteins, which are released by activated platelets. This creates a very narrow therapeutic window in which patients receiving a subtherapeutic dose have a high risk of reoccurring cardiac events and hemorrhaging in patients receiving too aggressive of therapy (Johnson 1994).

Surgical interventions for stenosis, or an abnormal narrowing of an artery due to atherosclerotic plaques, include percutaneous transluminal coronary angioplasty, bypass, or endarterectomy. Angioplasty is used to restore normal blood flow through the affected artery and involves inserting a balloon into the area of stenosed vessel and inflating it, compressing the atherosclerotic plaque. A bare metal stent can then be inserted into the vessel to maintain its patency, preventing recoil of the artery and provide a scaffold for regrowth of endothelial cells (Savage, Fischman et al. 1994; Serruys, de Jaegere et al. 1994). Unfortunately restenosis, or a 50% narrowing of the

vessel, occurs in about 40% of patients within 6 months after percutaneous transluminal angioplasty (Schillinger, Exner et al. 2003). Recently, drug eluting stents have helped reduce the risk of restenosis by reducing the proliferation of smooth muscle cells or enhancing the re-endothelialization of the vessel, both of which decrease the "scar" formation in the injured blood vessel (Finn, Nakazawa et al. 2007; Girod, Mulukutla et al. 2008). The process of restenosis is not fully understood though, and further refinements to the stents continue to be made, including changes in the stent material and what drugs are eluted (Waksman 2007).

An endarterectomy is usually performed to treat cerebrovascular disease, in which there is a serious reduction of blood supply to the brain (carotid endarterectomy), or to treat peripheral vascular disease (impaired blood supply to the legs). A blunt instrument is used to remove the intimal and medial layers of the blood vessel where the plaque is located. This procedure is very effective at returning blood flow through the vessel but there is still a risk of serious complications from the procedure including infection, stroke, bleeding, and blood clots (Vogel, Dombrovskiy et al. 2008). Therefore, this intervention is not performed unless symptoms are severe.

Bypass surgery is generally performed in patients with coronary occlusions in vessels on the surface of the heart or in other vessels that are too heavily damaged or calcified to perform reopening procedures. An alternate route for blood flow around the blockage is usually created by grafting healthy vessels from the patient's leg, arm, chest or abdomen or synthetic tubing into the vessel. In some instances, an artery is

redirected by cutting it and connecting it in another location where blood flow is more urgently needed because of lack of collateral blood flow. Serious complications can occur after bypass surgery including cognitive decline, stroke, or infection (Dieleman, Sauer et al. 2008). Current forms of both diagnosis and treatment for atherosclerosis have limitations in their effectiveness and have serious risks associated with them. Targeted delivery of imaging agents and therapeutics to atherosclerotic plaques could lead to more effective management of this complex disease.

### **Targeting atherosclerotic plaques**

Targeted delivery of diagnostic imaging agents and therapeutic drugs to atherosclerotic plaques is an ambitious goal in atherosclerotic research that is coming closer to a reality. Imaging dyes that are targeted to lesions give greater detail and information about the plaques and their morphology. Targeted delivery of currently available therapeutics such as anticoagulants to the atherosclerotic plaques would allow the drug to concentrate in the affected tissue, thereby enabling a lower dose and lowering the risk of side effects.

Recent advances in imaging techniques, especially magnetic resonance technology allow imaging of vessels at much higher resolution, even at the submillimeter level (Briley-Saebo, Mulder et al. 2007; Briley-Saebo, Shaw et al. 2008). Contrast agents for MRI, such as iron oxide or gadolinium, have been targeted toward activated platelets to monitor thrombus formation (von zur Muhlen, von Elverfeldt et al.

2008), or specific plaque components such as VCAM-1 (Kelly, Nahrendorf et al. 2006), oxLDL (Briley-Saebo, Shaw et al. 2008), and macrophages (Mulder, Strijkers et al. 2007), which allow non-invasive imaging of plaques in high detail. However, there is an urgent need to develop imaging techniques that can discriminate between stable plaques and those that are prone to rupture.

The goal of these experiments is to find new targeting elements that recognize atherosclerotic plaques, especially unstable plaques vulnerable to rupture, for delivery of diagnostic imaging agents and therapeutic drugs using nanoparticles. We analyzed various animal models of atherosclerosis for their utility in *in vivo* phage display using T7 phage to discover peptides that can recognize plaques which have ruptured or are prone to rupture. We also investigated the possibility of modifying R-Ras expression in plaques, leading to restructuring of the vulnerable plaque to induce stabilization. The T7 phage clone was optimized with mutations in the tail proteins which allowed the phage to circulate longer in the bloodstream. *In vivo* phage display was then used to test peptides that were developed to target tumors *in vivo* for their ability to recognize atherosclerotic plaques. One peptide identified from the screens to bind to plaques in the ApoE knockout mouse, CREKA, was then attached to micellar nanoparticles. CREKA targeted micelles coated the entire surface of the plaques, but concentrated in the shoulder regions of the plaque, which are more prone to rupture. These micelles recognized clotted plasma proteins on the plaque's surface and effectively delivered fluorescent dyes and an anticoagulant thrombin inhibitor to the plaques *in vivo*.

## References

- Amarenco, P. and A. M. Tonkin (2004). "Statins for stroke prevention: disappointment and hope." Circulation **109**(23 Suppl 1): III44-9.
- Blake, G. J. and P. M. Ridker (2002). "Inflammatory bio-markers and cardiovascular risk prediction." J Intern Med **252**(4): 283-94.
- Briley-Saebo, K. C., W. J. Mulder, V. Mani, F. Hyafil, V. Amirbekian, J. G. Aguinaldo, E. A. Fisher and Z. A. Fayad (2007). "Magnetic resonance imaging of vulnerable atherosclerotic plaques: current imaging strategies and molecular imaging probes." J Magn Reson Imaging **26**(3): 460-79.
- Briley-Saebo, K. C., P. X. Shaw, W. J. Mulder, S. H. Choi, E. Vucic, J. G. Aguinaldo, J. L. Witztum, V. Fuster, S. Tsimikas and Z. A. Fayad (2008). "Targeted molecular probes for imaging atherosclerotic lesions with magnetic resonance using antibodies that recognize oxidation-specific epitopes." Circulation **117**(25): 3206-15.
- Buffon, A., L. M. Biasucci, G. Liuzzo, G. D'Onofrio, F. Crea and A. Maseri (2002). "Widespread coronary inflammation in unstable angina." N Engl J Med **347**(1): 5-12.
- Carr, S., A. Farb, W. H. Pearce, R. Virmani and J. S. Yao (1996). "Atherosclerotic plaque rupture in symptomatic carotid artery stenosis." J Vasc Surg **23**(5): 755-65; discussion 765-6.
- CDC (1999). "From the Centers for Disease Control and Prevention. Ten great public health achievements--United States, 1900-1999." JAMA **281**(16): 1481.
- Cybulsky, M. I. and M. A. Gimbrone, Jr. (1991). "Endothelial expression of a mononuclear leukocyte adhesion molecule during atherogenesis." Science **251**(4995): 788-91.
- Dieleman, J., A. M. Sauer, C. Klijn, H. Nathoe, K. Moons, C. Kalkman, J. Kappelle and D. Van Dijk (2008). "Presence of coronary collaterals is associated with a decreased incidence of cognitive decline after coronary artery bypass surgery." Eur J Cardiothorac Surg.
- Finn, A. V., G. Nakazawa, M. Joner, F. D. Kolodgie, E. K. Mont, H. K. Gold and R. Virmani (2007). "Vascular responses to drug eluting stents: importance of delayed healing." Arterioscler Thromb Vasc Biol **27**(7): 1500-10.

- Fuster, V., Z. A. Fayad, P. R. Moreno, M. Poon, R. Corti and J. J. Badimon (2005). "Atherothrombosis and high-risk plaque: Part II: approaches by noninvasive computed tomographic/magnetic resonance imaging." J Am Coll Cardiol **46**(7): 1209-18.
- Fuster, V., P. R. Moreno, Z. A. Fayad, R. Corti and J. J. Badimon (2005). "Atherothrombosis and high-risk plaque: part I: evolving concepts." J Am Coll Cardiol **46**(6): 937-54.
- George, J. (2008). "Mechanisms of disease: the evolving role of regulatory T cells in atherosclerosis." Nat Clin Pract Cardiovasc Med **5**(9): 531-40.
- Girod, J. P., S. R. Mulukutla and O. C. Marroquin (2008). "Off-label use of stents: bare-metal versus drug-eluting stents." Expert Rev Cardiovasc Ther **6**(8): 1095-106.
- Herrick, J. B. (1983). "Landmark article (JAMA 1912). Clinical features of sudden obstruction of the coronary arteries. By James B. Herrick." JAMA **250**(13): 1757-65.
- Johnson, P. H. (1994). "Hirudin: clinical potential of a thrombin inhibitor." Annu Rev Med **45**: 165-77.
- Kelly, K. A., M. Nahrendorf, A. M. Yu, F. Reynolds and R. Weissleder (2006). "In vivo phage display selection yields atherosclerotic plaque targeted peptides for imaging." Mol Imaging Biol **8**(4): 201-7.
- Lamon, B. D. and D. P. Hajjar (2008). "Inflammation at the molecular interface of atherogenesis: an anthropological journey." Am J Pathol **173**(5): 1253-64.
- Law, M. R., N. J. Wald and A. R. Rudnicka (2003). "Quantifying effect of statins on low density lipoprotein cholesterol, ischaemic heart disease, and stroke: systematic review and meta-analysis." BMJ **326**(7404): 1423.
- Li, A. C. and C. K. Glass (2002). "The macrophage foam cell as a target for therapeutic intervention." Nat Med **8**(11): 1235-42.
- Libby, P. (2001). "Current concepts of the pathogenesis of the acute coronary syndromes." Circulation **104**(3): 365-72.
- Loftus, I. and M. Thompson (2008). "Plaque biology: interesting science or pharmacological treasure trove?" Eur J Vasc Endovasc Surg **36**(5): 507-16.



- Malle, E., G. Marsche, J. Arnhold and M. J. Davies (2006). "Modification of low-density lipoprotein by myeloperoxidase-derived oxidants and reagent hypochlorous acid." Biochim Biophys Acta **1761**(4): 392-415.
- Matsuura, E., K. Kobayashi, M. Tabuchi and L. R. Lopez (2006). "Oxidative modification of low-density lipoprotein and immune regulation of atherosclerosis." Prog Lipid Res **45**(6): 466-86.
- Mulder, W. J., G. J. Strijkers, K. C. Briley-Saboe, J. C. Frias, J. G. Aguinaldo, E. Vucic, V. Amirbekian, C. Tang, P. T. Chin, K. Nicolay and Z. A. Fayad (2007). "Molecular imaging of macrophages in atherosclerotic plaques using bimodal PEG-micelles." Magn Reson Med **58**(6): 1164-70.
- Napoli, C., F. P. D'Armiento, F. P. Mancini, A. Postiglione, J. L. Witztum, G. Palumbo and W. Palinski (1997). "Fatty streak formation occurs in human fetal aortas and is greatly enhanced by maternal hypercholesterolemia. Intimal accumulation of low density lipoprotein and its oxidation precede monocyte recruitment into early atherosclerotic lesions." J Clin Invest **100**(11): 2680-90.
- Palinski, W. and S. Tsimikas (2002). "Immunomodulatory effects of statins: mechanisms and potential impact on arteriosclerosis." J Am Soc Nephrol **13**(6): 1673-81.
- Rosamond, W., K. Flegal, G. Friday, K. Furie, A. Go, K. Greenlund, N. Haase, M. Ho, V. Howard, B. Kissela, S. Kittner, D. Lloyd-Jones, M. McDermott, J. Meigs, C. Moy, G. Nichol, C. J. O'Donnell, V. Roger, J. Rumsfeld, P. Sorlie, J. Steinberger, T. Thom, S. Wasserthiel-Smoller and Y. Hong (2007). "Heart disease and stroke statistics--2007 update: a report from the American Heart Association Statistics Committee and Stroke Statistics Subcommittee." Circulation **115**(5): e69-171.
- Ruffer, M. (1911). "On arterial lesions found in Egyptian mummies." J Pathol Bacteriol **15**: 453-462.
- Ruffer, M. (1920). "Remarks on the histology and pathological anatomy of Egyptian mummies." Cairo Scientific J **4**: 3-7.
- Savage, M. P., D. L. Fischman, R. A. Schatz, P. S. Teirstein, M. B. Leon, D. Baim, S. G. Ellis, E. J. Topol, J. W. Hirshfeld, M. W. Cleman and et al. (1994). "Long-term angiographic and clinical outcome after implantation of a balloon-expandable stent in the native coronary circulation. Palmaz-Schatz Stent Study Group." J Am Coll Cardiol **24**(5): 1207-12.

- Schillinger, M., M. Exner, W. Mlekusch, M. Haumer, S. Sabeti, R. Ahmadi, I. Schwarzwinger, O. Wagner and E. Minar (2003). "Restenosis after femoropopliteal PTA and elective stent implantation: predictive value of monocyte counts." J Endovasc Ther **10**(3): 557-65.
- Schonbeck, U. and P. Libby (2004). "Inflammation, immunity, and HMG-CoA reductase inhibitors: statins as antiinflammatory agents?" Circulation **109**(21 Suppl 1): II18-26.
- Serruys, P. W., P. de Jaegere, F. Kiemeneij, C. Macaya, W. Rutsch, G. Heyndrickx, H. Emanuelsson, J. Marco, V. Legrand, P. Materne and et al. (1994). "A comparison of balloon-expandable-stent implantation with balloon angioplasty in patients with coronary artery disease. Benestent Study Group." N Engl J Med **331**(8): 489-95.
- Stary, H. C., A. B. Chandler, S. Glagov, J. R. Guyton, W. Insull, Jr., M. E. Rosenfeld, S. A. Schaffer, C. J. Schwartz, W. D. Wagner and R. W. Wissler (1994). "A definition of initial, fatty streak, and intermediate lesions of atherosclerosis. A report from the Committee on Vascular Lesions of the Council on Arteriosclerosis, American Heart Association." Arterioscler Thromb **14**(5): 840-56.
- Virmani, R., A. P. Burke, F. D. Kolodgie and A. Farb (2003). "Pathology of the thin-cap fibroatheroma: a type of vulnerable plaque." J Interv Cardiol **16**(3): 267-72.
- Virmani, R., F. D. Kolodgie, A. P. Burke, A. Farb and S. M. Schwartz (2000). "Lessons from sudden coronary death: a comprehensive morphological classification scheme for atherosclerotic lesions." Arterioscler Thromb Vasc Biol **20**(5): 1262-75.
- Vogel, T. R., V. Y. Dombrovskiy, P. B. Haser, J. C. Scheirer and A. M. Graham (2008). "Carotid stenting and endarterectomy in the United States: Age and outcomes." J Vasc Surg.
- von zur Muhlen, C., D. von Elverfeldt, J. A. Moeller, R. P. Choudhury, D. Paul, C. E. Hagemeyer, M. Olschewski, A. Becker, I. Neudorfer, N. Bassler, M. Schwarz, C. Bode and K. Peter (2008). "Magnetic resonance imaging contrast agent targeted toward activated platelets allows in vivo detection of thrombosis and monitoring of thrombolysis." Circulation **118**(3): 258-67.
- Waksman, R. (2007). "Promise and challenges of bioabsorbable stents." Catheter Cardiovasc Interv **70**(3): 407-14.

Yla-Herttuala, S., B. A. Lipton, M. E. Rosenfeld, T. Sarkioja, T. Yoshimura, E. J. Leonard, J. L. Witztum and D. Steinberg (1991). "Expression of monocyte chemoattractant protein 1 in macrophage-rich areas of human and rabbit atherosclerotic lesions." Proc Natl Acad Sci U S A **88**(12): 5252-6.

## Chapter 2

### **Animal models of atherosclerosis**

#### **Abstract**

Atherosclerosis is a complex disease that takes years to develop in humans and has been difficult to duplicate in an animal model. It results from interactions of multiple genetic and environmental factors including diet and defects in lipid metabolism. Many aspects of the human disease have been replicated in animal models but an atherosclerotic animal model that is easy to use and encompasses the full progression of the disease from the development of advanced lesions in the arterial walls to thrombosis formation leading to myocardial infarction and death has remained elusive. Two animal models of atherosclerosis were studied to determine if they could be used to identify novel targeting peptides for lesions that were vulnerable to rupture and a new animal model was developed to study the stabilization of vulnerable plaques.

#### **Introduction**

Atherosclerosis, one of the leading causes of death in the United States each year, has many genetic factors which have been identified to be involved in its progression (Acton, Go et al. 2004). These genetic changes, especially the ones involved in lipid metabolism, have been utilized by researchers to develop multiple transgenic animal models that reproduce some of the same characteristics as human

atherosclerosis. Apolipoproteins regulate lipoprotein metabolism through their involvement in the transport and redistribution of lipids between various cells and tissues (Mahley, Innerarity et al. 1984). Apolipoprotein E (ApoE), one of the main classes of apoprotein, is a glycoprotein that is about 34 kD and is expressed in both mice and humans. It is a high affinity ligand for the low density lipoprotein (LDL) receptor and is essential for normal lipoprotein metabolism and excretion. Variants of the ApoE gene in humans, ApoE2 and ApoE4 specifically, cause familial type III hyperlipoproteinemia, increased risk of atherosclerosis, and late-onset Alzheimer's disease (Mahley 1988; Strittmatter and Roses 1995). In 1992, with the advent of gene knockout technology, an ApoE knockout mouse model of atherosclerosis was developed (Piedrahita, Zhang et al. 1992). This model is one of the most widely used animal models in atherosclerosis research. Lesions reproducibly develop in these mice in the aortic sinus, aortic arch, and each of the branch points along the aorta. Signs of plaque rupture have also been observed in the brachiocephalic arteries of these mice when they are fed a high fat diet (Johnson, Carson et al. 2005; Jackson, Bennett et al. 2007). ApoE knockout mice fed a high fat diet have been used in previous studies to develop targeting peptides for atherosclerotic plaques (Houston, Goodman et al. 2001; Liu, Bhattacharjee et al. 2003; Kelly, Nahrendorf et al. 2006), but no previous studies have tried to find peptides that target plaques vulnerable to rupture.

ApoE knockout mice on a high fat diet develop advanced atherosclerotic plaques similar to the human disease but other clinical manifestations of atherosclerosis, such as unstable angina and acute myocardial infarction (MI) are not present in this

model. In order to try and replicate some of these symptoms, a transgenic mouse with the gene that codes for the scavenger receptor class B type I (SR-BI) knocked out was crossed with the ApoE knockout mouse (Braun, Trigatti et al. 2002). This scavenger receptor is involved in hepatocyte uptake and macrophage efflux of cholesterol and is crucial in the reverse cholesterol transport pathway. ApoE/SR-BI double knockout mice (dKO) develop severe hypercholesterolemia and similar defects to those seen in human coronary heart disease, including MI and death. All of these mice die between 5-8 weeks of age and show signs of thrombus formation and evidence of previous MIs at death. This model of atherosclerosis was acquired and bred to determine its suitability in screens for vulnerable plaques and it also was used to study the stabilization of lesions that are vulnerable to rupture.

R-Ras is a low molecular weight GTPase that shares 50% homology with the other Ras family of proteins (H-, K-, and N-Ras) (Lowe, Capon et al. 1987) and has been shown to activate integrins and enhance cell adhesion (Zhang, Vuori et al. 1996). It has been shown to be involved in mediating the adhesion of monocytes to activated endothelial cells, one of the primary factors in the initiation and progression of atherosclerotic plaques, thus starting an inflammatory reaction in the injured arterial wall. Expression of R-Ras has also been shown to have an effect on the regulation of smooth muscle cells that reside in the medial layer of the arterial wall. Over-expression in cultured smooth muscle cells has been shown to inhibit proliferation and migration.

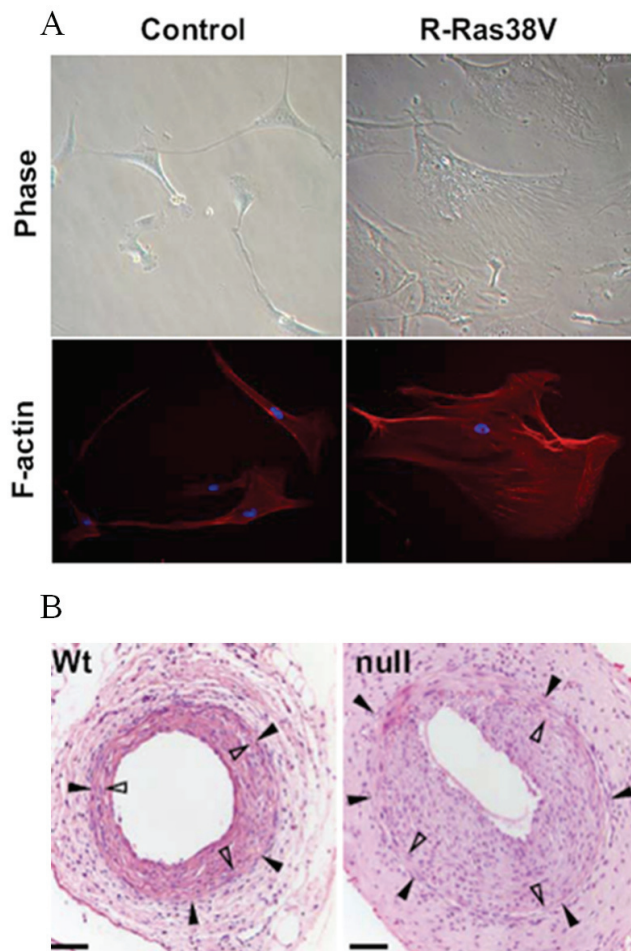


**Figure 2.1:** Effect of R-Ras on smooth muscle cell attachment and intimal hyperplasia. (A) Cultured smooth muscle cells exhibit more attachment and spreading when transfected with a constitutively active form of R-Ras (R-Ras38V). (B) Increased intimal hyperplasia is seen in R-Ras knockout mice compared to wild-type mice following arterial injury in which the endothelial layer is removed. (*Reproduced with permission (Komatsu and Ruoslahti 2005).*)

Loss of R-Ras *in vivo* had the reverse effect and caused increased smooth muscle cell migration and proliferation, inducing intimal hyperplasia after arterial injury (Fig 2.1) (Komatsu and Ruoslahti 2005). The role of R-Ras in many of the processes involved with the progression of atherosclerosis and remodeling of plaques led us to look at whether disruption in the expression of this protein could be utilized to cause the

stabilization of the vulnerable atherosclerotic plaques seen in the ApoE/SR-BI mouse model and lead to an increased survival time.

## **Methods**

**ApoE knockout mice.** Mice homozygous for the *ApoE*<sup>tm1Unc</sup> mutation were acquired from Jackson Labs (Bar Harbor, Maine). These mice were housed and bred according to standards of the University of California, Santa Barbara Institutional Animal Care and Use Committee. At 3 weeks of age, pups were separated from their mothers and switched to a high fat diet (42% fat, TD88137, Harlan, Madison, WI) for 6 months to generate stage V lesions in the major vessels (Whitman 2004). Mice were anesthetized for procedures with a ketamine-xylazine cocktail (80-100mg/kg and 5-10mg/kg, respectively) intraperitoneally and monitored using a toe pinch with more anesthetic given as needed. Blood was collected from the orbital sinus of mice and total plasma cholesterol levels were determined using the Wako Cholesterol E enzymatic colorimetric method (Wako Diagnostics, Richmond, VA).

Anesthetized mice were perfused through the left ventricle with 40ml cold Dulbecco's Modified Eagle's Medium (DMEM) to remove the blood from the circulatory system followed by 10ml 4% paraformaldehyde with quality of perfusion monitored by clearing of the saphenous vein. The aortic tree and heart were excised and fixed overnight in 4% paraformaldehyde, washed in phosphate buffered saline (PBS) and then put in a 30% sucrose solution for 8 hours. Sections of the aortic tree



containing atherosclerotic lesions and the heart were frozen in OCT and sectioned in 5µm sections on silane-coated slides (Scientific Device Laboratory, Des Plaines, IL) for histology. Smooth muscle actin in tissue sections was visualized using a polyclonal rabbit antibody against smooth muscle actin (1:100 dilution, Thermo Scientific Lab Vision, Fremont, CA) and goat, anti-rabbit Alexa Fluor 647 conjugated secondary antibody (Invitrogen, Carlsbad, CA). Slides were mounted and nuclei were visualized with ProLong Gold Antifade reagent with DAPI (Invitrogen, Carlsbad, CA). Immunofluorescence pictures were taken on a confocal microscope.

**ApoE/SR-BI double knockout mice.** B6;129-*Srb1*<sup>tm1Kri</sup> *ApoE*<sup>tm1Unc</sup> transgenic mice were acquired from the lab of Dr. Monty Krieger (Massachusetts Institute of Technology). ApoE homozygous null, SR-BI heterozygous mice were bred to generate double knockout mice because double homozygous null mice did not live long enough to breed. Tail clips were taken at three weeks of age and genomic DNA was isolated using a DNeasy Blood & Tissue Kit (Qiagen, Valencia, CA). Two separate PCR reactions were performed to determine the presence of a wild-type gene or a disrupted gene and the products were run a 2% agarose gel to determine SR-BI genotype. The genotyping protocol given by Jackson Labs for the mouse strain was altered by adding 5% DMSO and 0.1% BSA to the PCR mix. Tissue for histology was collected as described above. The aortic tree was stained for the presence of lipids in the vessel wall (fatty streaks) using Oil Red O. Sections of the heart were stained with hematoxylin

and eosin to look for the presence of acellular thrombus formation in the coronary arteries.

**ApoE/SR-BI/R-Ras triple knockout.** ApoE/SR-BI double knockout mice were crossed with R-Ras knockout mice to generate the ApoE/SR-BI/R-Ras triple knockout. Both lines had previously been backcrossed into the C57BL/6 strain. A stable line of ApoE null, R-Ras null, SR-BI heterozygous was generated for breeding of the triple knockout because mice homozygous null for the SR-BI gene do not breed well (Rigotti, Trigatti et al. 1997). In order to determine the genotype for the mice of each gene, a tail clip was taken at 3 weeks of age and genomic DNA was isolated. The standard PCR protocol for genotyping ApoE knockout mice (Jackson Labs website) was used as well as the modified protocol for genotyping SR-BI knockout mice described above. A new PCR protocol had to be derived to determine the R-Ras gene though because all three gene disruptions used a neomycin cassette. The presence of this cassette was originally what was used to determine the presence of the disrupted gene. PCR primer pairs were determined that could identify the wild-type R-Ras gene (5'-GGAACAAGGCAGATCTGG-3', 5'-AAGAGGAGGCTTCAGACC-3') and the disrupted R-Ras gene (5'-ACCGAGCTGCAAGAAGCTTCTCCTCA-3' and 5'-AGGAGGCCTTCCATCTGTTGCT). PCR products were run on 2% agarose gels to determine genotype with a 550bp band signifying the wild-type gene and a 210bp band signifying the disrupted allele.

ApoE/SR-BI/R-Ras mice were watched for signs of distress and death and the number of days each mouse was alive was plotted compared to the published survival times of the ApoE/SR-BI double knockout mice (Braun, Trigatti et al. 2002).

## Results

**ApoE knockout mice.** ApoE knockout mice that were placed on a high fat diet became severely obese after only 16 weeks compared to wild-type mice on a normal diet (48g and 20g, respectively, Fig 2.2A). Cholesterol levels in the blood were significantly higher in the ApoE null mice on a standard chow diet (6.5mg/ml for ApoE null mice and 0.475mg/ml for wild-type mice), with even higher levels when these mice were fed a high fat diet (9.5mg/ml, Fig 2.2B). The aortic tree and heart were excised in ApoE knockout and wild-type mice to determine if atherosclerotic plaques had formed in their blood vessels. Large plaques were consistently seen in the cross-sections of the aortic arch and the three major branches off of the aorta, especially the brachiocephalic

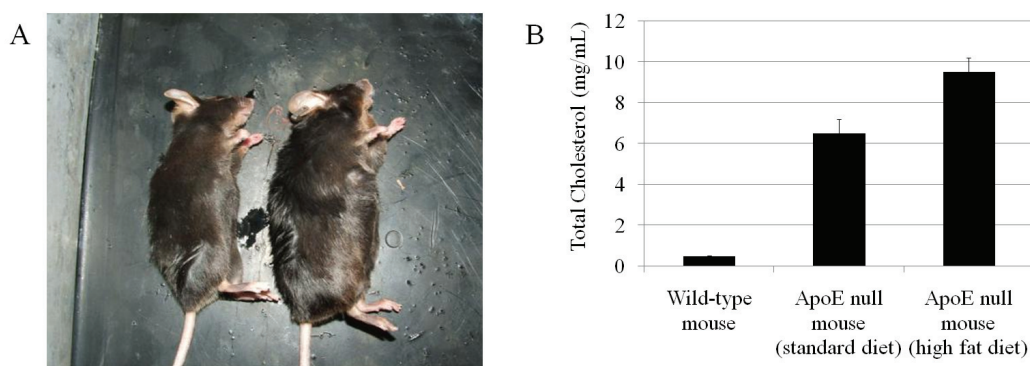


**Figure 2.2:** ApoE null mouse model of atherosclerosis. (A) Wild-type (left, 20g) and ApoE null mouse fed high fat diet for 16 weeks (right, 48g). (B) Total blood cholesterol in wild-type, ApoE null, and ApoE null mouse on a high fat diet (Error bars represent standard error of the mean, n=3).

artery, of ApoE mice fed a high fat diet for 6 months. Plaques were not seen in any wild-type mice of similar age (Figure 2.3A, B). These lesions protrude into the lumen of the vessel, decreasing the area for blood flow. Plaques in the coronary arteries of ApoE null mice have been reported in older mice on a high fat diet for 9-20 months (Calara, Silvestre et al. 2001), but are not consistently produced and were not seen in any of our mice after 6 months on a high fat diet. Aortic sections were stained with antibodies against smooth muscle actin to determine how advanced the atherosclerotic lesions were. Buried fibrous caps can be seen in the immunofluorescence pictures

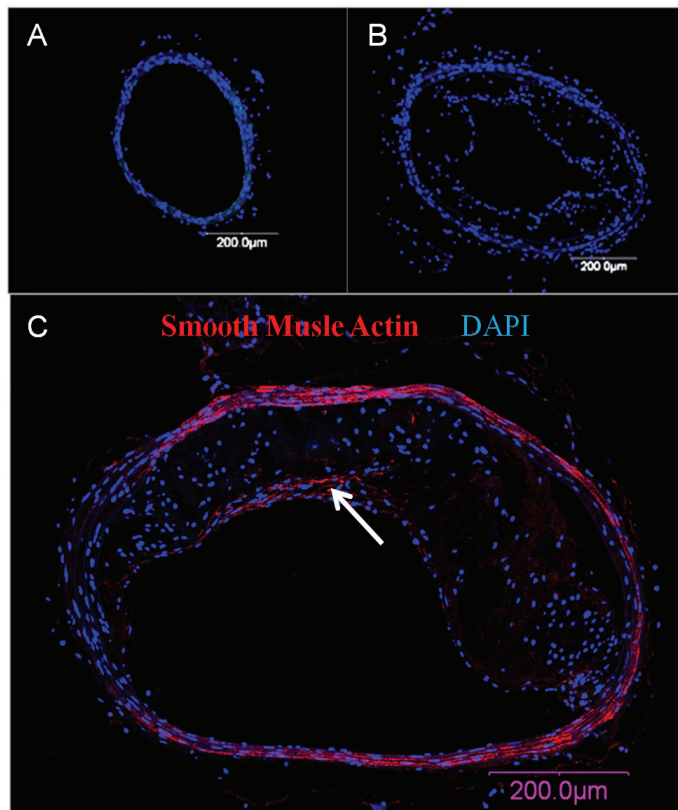


**Figure 2.3:** Morphology of plaques in ApoE null mice. Tissue cross-sections (5 $\mu$ m thick) of the brachiocephalic artery were cut with from wildtype (A) and ApoE null mice fed a high fat diet for 6 months (B, C). Nuclei are stained with DAPI in blue. (C) Buried fibrous caps were visualized in the advanced lesions of ApoE null mice on a high fat diet (white arrow).

(Figure 2.3C, white arrow), which is a sign of previous plaque rupture. ApoE null mice on a high fat diet have high blood cholesterol levels and consistently develop atherosclerotic lesions in the large vessels that are easy to access and study.

**ApoE/SR-BI double knockout mice.** Mice homozygous null for the ApoE and SR-BI genes develop signs of severe coronary atherosclerosis at around 5 weeks of age on a normal chow diet and all of the mice die at 5-8 weeks of age. Aortas of wild-type and ApoE/SR-BI dKO mice were excised and stained with Oil Red O, which stains lipids that are present in the vessel wall. ApoE/SR-BI dKO mice (Figure 2.4A, left) had already developed fatty streaks in their large vessels at 6 weeks which were not present in the vessels of wild-type mice (Figure 2.4A, right). Mice generally started to show severe distress within a couple of hours prior to death and their hearts showed signs of scar formation from previous myocardial infarction in necropsy (Figure 2.4B, white arrow). Acellular blockages in the coronary arteries of the deceased mice were also seen in histological sections of the heart (Figure 2.4C, black arrows).

**ApoE/SR-BI/R-Ras triple knockout mice.** ApoE/SR-BI dKO mice were crossed with R-Ras null mice to determine if loss of R-Ras could prolong the lifespan of the double knockout mice, possibly through the stabilization of the coronary plaques. A new genotyping protocol was devised for the triple knockout because the standard protocol for genotyping R-Ras transgenic mice used primers which recognize the neomycin cassette that was inserted into the R-Ras gene in the creation of the knockout

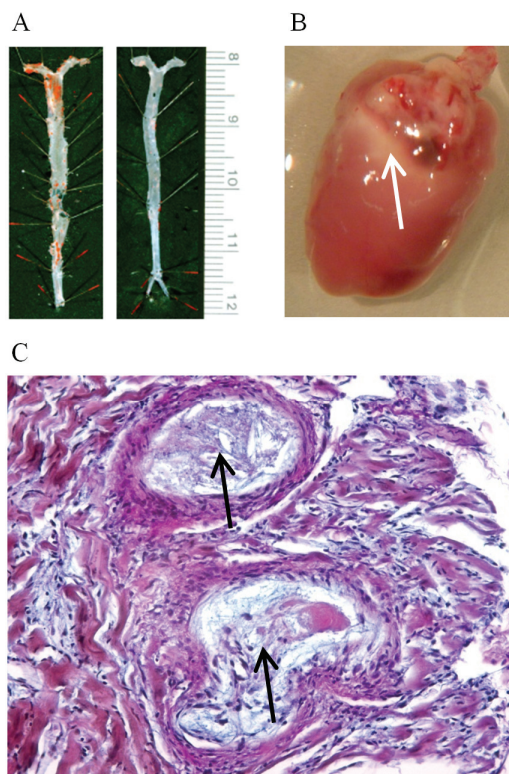


**Figure 2.4:** ApoE/SRBI double knockout model of atherosclerosis. Mice null for both the ApoE and SR-BI proteins developed fatty streaks in their aorta and thromboses in their coronary arteries in as little as 5 weeks after birth on a standard chow diet, and died of myocardial infarction at 5-8 weeks of age. (A) Aortic tree stained for lipids with Oil Red O. Fatty streaks in the wall of the vessel are apparent in the aorta of the ApoE/SR-BI null mouse (left) but not the wildtype (right). (B) Evidence of previous myocardial infarction in heart from ApoE/SR-BI null mouse. White arrow points to scar tissue. (C) Histological section of heart from ApoE/SR-BI mouse. Acellular thrombi are evident in the left anterior descending and circumflex coronary arteries of the heart (black arrows).

mouse. The same technique of inserting a neomycin cassette was also used in the disruption of both the ApoE and SR-BI genes and so new primers that were unique for the disrupted R-Ras gene had to be derived. Importantly, the new PCR protocols were able to differentiate between homozygous null, heterozygous, and homozygous wild-type for each of the three genes in the same mouse (Figure 2.5). Mice that were homozygous null for all three genes lived significantly longer than the previously

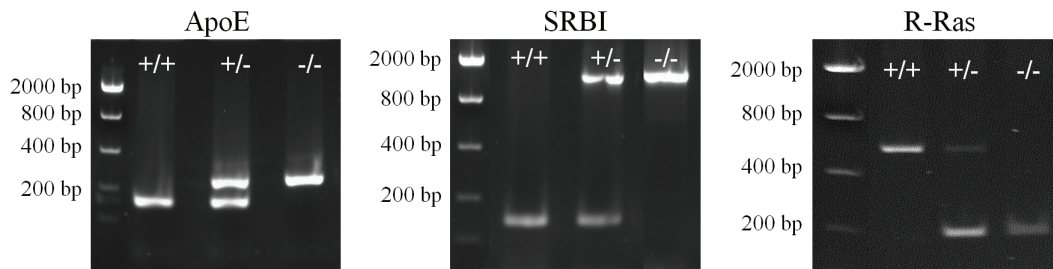


**Figure 2.5** Genotyping ApoE/SR-BI/R-Ras triple knockout mice. Genomic DNA was isolated from tail clips of mice. Separate PCR reactions were performed to determine the genotype for each gene and the PCR products were run on a 2% agarose gel.

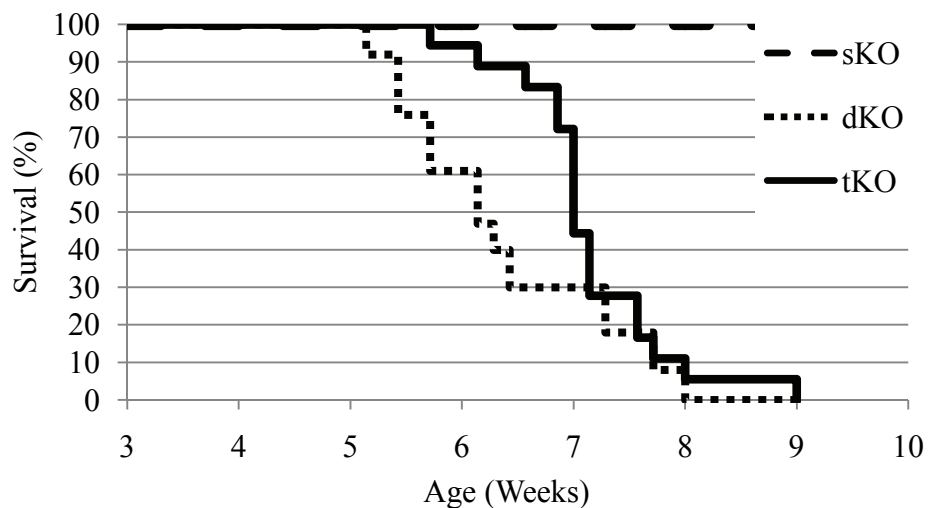


**Figure 2.6:** Survival curve of ApoE null (sKO), ApoE/SR-BI null (dKO), and ApoE/SR-BI/R-Ras null (tKO) mice. sKO mice on a high fat diet do not have a decreased life span. tKO mice had a significantly longer lifespan than dKO mice, 49 and 43 days, respectively ( $p \leq 0.05$ ,  $n=17$  mice for tKO and 19 mice for dKO).

reported lifespan of ApoE/SR-BI double knockout mice (49 and 43 days,  $p \leq 0.05$ ,

Figure 2.6).

## Discussion

ApoE knockout mice are one of the most widely studied mouse models of atherosclerosis. They have multiple positive and negative factors in their use for *in vivo*

*phage* screening to isolate targeting peptides that specifically recognize atherosclerotic lesions vulnerable to rupture. One positive factor is these mice reproducibly start to develop plaques very quickly on a high fat diet in characteristic places in the vasculature. They have even been reported to have evidence of plaque rupture in the brachiocephalic artery in as little as 8 weeks on a high fat diet (Johnson, Carson et al. 2005). On the other hand, these advanced lesions take much longer to be consistently produced in the vasculature. Mice must be on a high fat diet for at least 6 months to a year to be confident that the mice will have large stage V plaques. The tissue that contains the atherosclerotic plaques, the aortic tree, is also very small and therefore tissue from multiple mice needs to be pooled together for each round of screening. This makes the breeding and upkeep of these mice very expensive for the large numbers that are needed for phage screening with randomized libraries.

Alternatively, ApoE null mice on a high fat diet are a great model of atherosclerosis for confirmation of the targeting peptide's homing capability with peptides, nanoparticles, or individual phage clones. Fewer mice are needed for confirmation than for screens. Also, large advanced plaques are generated throughout the vasculature, and it is fairly easy to isolate regions of the aortic tree that contain plaques macroscopically, which is necessary in order to cut histological sections.

The ApoE/SR-BI double knockout mouse seems to be a very good mouse model of coronary atherosclerosis that leads to thrombosis. Double knockout mice develop many of the same features of human coronary artery disease including hypercholesterolemia, occlusive coronary atherosclerosis, spontaneous myocardial



infarction, cardiac dysfunction (ECG abnormalities, heart enlargement, and reduced systolic function), and early death, that are not seen in other atherosclerotic animal models (Braun, Trigatti et al. 2002). Mice develop the disease extremely quickly (5-8 weeks of age), so it is faster to generate diseased mice for study with this model than the ApoE single knockout mice. Unfortunately, these mice are very young, small, sick, and difficult to work with. Many of the mice die during restraint or anesthesia before any experiments can be performed. The complications from the loss of both the ApoE and SR-BI proteins develop so quickly that these mice cannot be bred homozygously, and therefore only 25% of the mice that are bred have the needed genotype. It is also too fast for large plaques to develop in the major blood vessels. Fatty streaks can be seen in the aortic tree with lipid staining, but this is a very early stage of plaque development. The plaques that seem to rupture are in the coronary arteries and these small vessels are difficult to access and isolate.

Recently, alterations to the ApoE/SR-BI double knockout mouse model have been made that extend the lifespan of the animals and should make the model easier to work with. Probucol, an anti-atherosclerosis lipid lowering drug, extended the lifespan of the double knockout mice to as long as 60 weeks (Braun, Zhang et al. 2003). A diet inducible ApoE/SR-BI dKO model also now exists. SR-BI knockout mice were crossed with a hypomorphic ApoE mouse that expresses reduced levels of an ApoE4-like murine ApoE isoform (Zhang, Picard et al. 2005). The mice do not develop the severe symptoms of the ApoE/SR-BI mice when they are fed a normal chow diet, but develop similar symptoms with a 50% mortality rate around 5 weeks after they are changed to a

high fat diet. This model could allow better control over the timing of when mice develop symptoms so that they are older, bigger, and easier to work with when a phage screen is performed.

ApoE/SR-BI double knockout mice were crossed with R-Ras null mice to see if the phenotype of the dKO mice could be rescued and the lifespan prolonged. R-Ras single knockout mice do not exhibit an obvious phenotype or a shortened lifespan but the protein has been shown to be involved with monocyte adhesion to oxidized LDL activated endothelial cells and regulation of smooth muscle cell proliferation and migration. It was thought that knocking out R-Ras might have a two-pronged effect that could stabilize the atherosclerotic plaques that appear to be rupturing causing the thrombosis and death in the dKO. The ApoE/SR-BI/R-Ras triple knockout mice have a statistically significant, slightly prolonged lifespan compared to the dKO mice, demonstrating that regulation of R-Ras in plaques vulnerable to rupture could have a protective effect. Decreased R-Ras expression has been shown to promote proliferation and migration of smooth muscle cells which secrete matrix proteins needed for the fibrous structure of a stable plaque. It could also help decrease the deposition of lipid in the plaque if fewer monocytes were able to adhere and extravasate into the plaque.

## References

- Acton, R. T., R. C. Go and J. M. Roseman (2004). "Genetics and cardiovascular disease." *Ethn Dis* **14**(4): S2-8-16.
- Braun, A., B. L. Trigatti, M. J. Post, K. Sato, M. Simons, J. M. Edelberg, R. D. Rosenberg, M. Schrenzel and M. Krieger (2002). "Loss of SR-BI expression leads to the early onset of occlusive atherosclerotic coronary artery disease,

spontaneous myocardial infarctions, severe cardiac dysfunction, and premature death in apolipoprotein E-deficient mice." Circ Res **90**(3): 270-6.

Braun, A., S. Zhang, H. E. Miettinen, S. Ebrahim, T. M. Holm, E. Vasile, M. J. Post, D. M. Yoerger, M. H. Picard, J. L. Krieger, N. C. Andrews, M. Simons and M. Krieger (2003). "Probucol prevents early coronary heart disease and death in the high-density lipoprotein receptor SR-BI/apolipoprotein E double knockout mouse." Proc Natl Acad Sci U S A **100**(12): 7283-8.

Calara, F., M. Silvestre, F. Casanada, N. Yuan, C. Napoli and W. Palinski (2001). "Spontaneous plaque rupture and secondary thrombosis in apolipoprotein E-deficient and LDL receptor-deficient mice." J Pathol **195**(2): 257-63.

Houston, P., J. Goodman, A. Lewis, C. J. Campbell and M. Braddock (2001). "Homing markers for atherosclerosis: applications for drug delivery, gene delivery and vascular imaging." FEBS Lett **492**(1-2): 73-7.

Jackson, C. L., M. R. Bennett, E. A. Biessen, J. L. Johnson and R. Krams (2007). "Assessment of Unstable Atherosclerosis in Mice." Arterioscler Thromb Vasc Biol.

Johnson, J., K. Carson, H. Williams, S. Karanam, A. Newby, G. Angelini, S. George and C. Jackson (2005). "Plaque rupture after short periods of fat feeding in the apolipoprotein E-knockout mouse: model characterization and effects of pravastatin treatment." Circulation **111**(11): 1422-30.

Kelly, K. A., M. Nahrendorf, A. M. Yu, F. Reynolds and R. Weissleder (2006). "In vivo phage display selection yields atherosclerotic plaque targeted peptides for imaging." Mol Imaging Biol **8**(4): 201-7.

Komatsu, M. and E. Ruoslahti (2005). "R-Ras is a global regulator of vascular regeneration that suppresses intimal hyperplasia and tumor angiogenesis." Nat Med **11**(12): 1346-50.

Liu, C., G. Bhattacharjee, W. Boisvert, R. Dilley and T. Edgington (2003). "In vivo interrogation of the molecular display of atherosclerotic lesion surfaces." Am J Pathol **163**(5): 1859-71.

Lowe, D. G., D. J. Capon, E. Delwart, A. Y. Sakaguchi, S. L. Naylor and D. V. Goeddel (1987). "Structure of the human and murine R-ras genes, novel genes closely related to ras proto-oncogenes." Cell **48**(1): 137-46.

Mahley, R. W. (1988). "Apolipoprotein E: cholesterol transport protein with expanding role in cell biology." Science **240**(4852): 622-30.

- Mahley, R. W., T. L. Innerarity, S. C. Rall, Jr. and K. H. Weisgraber (1984). "Plasma lipoproteins: apolipoprotein structure and function." J Lipid Res **25**(12): 1277-94.
- Piedrahita, J. A., S. H. Zhang, J. R. Hagaman, P. M. Oliver and N. Maeda (1992). "Generation of mice carrying a mutant apolipoprotein E gene inactivated by gene targeting in embryonic stem cells." Proc Natl Acad Sci U S A **89**(10): 4471-5.
- Rigotti, A., B. L. Trigatti, M. Penman, H. Rayburn, J. Herz and M. Krieger (1997). "A targeted mutation in the murine gene encoding the high density lipoprotein (HDL) receptor scavenger receptor class B type I reveals its key role in HDL metabolism." Proc Natl Acad Sci U S A **94**(23): 12610-5.
- Strittmatter, W. J. and A. D. Roses (1995). "Apolipoprotein E and Alzheimer disease." Proc Natl Acad Sci U S A **92**(11): 4725-7.
- Whitman, S. C. (2004). "A practical approach to using mice in atherosclerosis research." Clin Biochem Rev **25**(1): 81-93.
- Zhang, S., M. H. Picard, E. Vasile, Y. Zhu, R. L. Raffai, K. H. Weisgraber and M. Krieger (2005). "Diet-induced occlusive coronary atherosclerosis, myocardial infarction, cardiac dysfunction, and premature death in scavenger receptor class B type I-deficient, hypomorphic apolipoprotein ER61 mice." Circulation **111**(25): 3457-64.
- Zhang, Z., K. Vuori, H. Wang, J. C. Reed and E. Ruoslahti (1996). "Integrin activation by R-ras." Cell **85**(1): 61-9.

## Chapter 3

### **Discovering new atherosclerotic plaque-targeting ligands**

#### **using *in vivo* phage display**

##### **Abstract**

Phage display using T7 phage is a powerful technique used both *in vitro* and *in vivo* to find peptides that specifically bind to various proteins and surfaces. The T7 phage vector was optimized to increase the circulation time of the phage by introducing two mutations into the tail proteins of the phage that decreased their uptake by the liver. Phage display was also used to test various known homing peptides that bind to the vasculature of tumors to find peptides that also bind to atherosclerotic plaques.

##### **Introduction**

Phage display has been shown to be a very powerful tool to isolate short peptide sequences that bind with high specificity to a target molecule (Smith 1985; Smith and Petrenko 1997). With recombinant DNA technology peptide sequences are cloned into the bacteriophage DNA that codes for various proteins in the capsid. Randomized DNA inserts are cloned into the phage genome and used to generate phage libraries with enormous diversity of fusion peptides displayed on their surface. The individual peptides on the surface of each phage match the DNA sequence that was cloned into that specific phage, using biology to create a built in cipher to decrypt peptide sequences and allowing both the peptide or protein and its coding sequence to be

selected at the same time. Phage display has been used *in vitro* to select peptides with high binding affinities to various proteins and receptors and even inorganic materials (Kehoe and Kay 2005).

The technology has also been used *in vivo* to demonstrate the extensive heterogeneity in the vascular beds of different organs and to find peptides that can discriminate between diseased and normal tissue (Pasqualini and Ruoslahti 1996; Hoffman, Giraudo et al. 2003; Kelly, Nahrendorf et al. 2006). Most of the *in vivo* phage display performed utilizes the M13 filamentous phage as the phage vector. Phage display using T7 phage offers many advantages over M13 phage. T7 phage is a lytic phage and the completion of amplification is easily observed when the culture clears and loses turbidity. The phage are small, around 55nm in diameter, and can display anywhere from 1 to 415 copies of a peptide, up to 1000 amino acids in length as a C-terminal fusion to the capsid protein on the phage surface (Figure 3.1A). T7 also remains infective in a variety of eluting conditions such as in the presence of detergents, high molar urea and sodium chloride, and reducing or alkaline conditions (Rosenberg, Griffin et al. 1996). The process of an *in vivo* phage display screen works by injecting a random phage library with up to  $10^8$  different displayed peptides into a mouse and letting it circulate and bind to the vascular beds. The tissue of interest is then isolated and the bound phage are eluted and amplified. The amplified library is then injected into another mouse and the process is repeated. Multiple rounds of selection are performed until a highly enriched pool of phage that bind to your tissue of interest is isolated (Figure 3.1B).

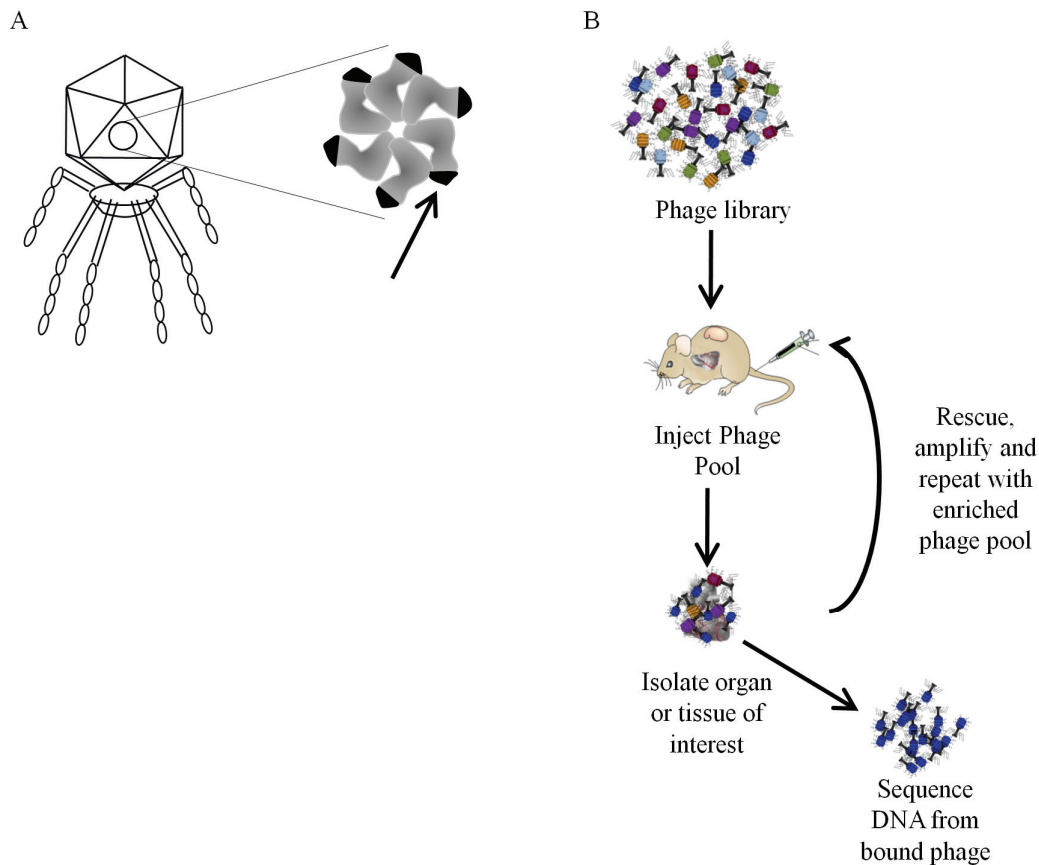


**Figure 3.1:** *In vivo* phage display using T7 phage library. (A) Structure of T7 phage. T7 is an icosahedral phage made up of 415 capsid proteins arranged in 60 hexamers at the faces and 11 pentamers at the vertices making up the capsid. Attached to the capsid is a head-tail connector, a short conical tail, and six tail proteins. A randomized DNA sequence is spliced into the end of the capsid gene (gene 10). The randomized peptide is expressed at the c-terminal end of each of the 415 capsid proteins (black arrow). (B) Schematic of *in vivo* phage display. A randomized library of T7 phage is injected into a mouse and allowed to circulate. The mouse is perfused to remove unbound phage and the tissue of interest is collected. Bound phage are rescued, amplified and injected into another animal for further selection. After multiple rounds of selection enriched phage pool is sequenced to determine peptides that bind to the tissue of interest.

A major limitation of using T7 phage in *in vivo* phage display is the very short half-life of phage in the circulation. The phage are quickly cleared with a half-life of around 12 minutes, which results in only 3% of the injected phage still circulating after one hour (Fan, Venegas et al. 2007). This rapid loss of phage could lead to peptide

candidates being cleared from the circulation before they even reach their target tissue. Recently, two separate mutations in gene 17 of T7 phage were discovered that reduced uptake of the particles by hepatocytes in the liver (Sokoloff, Wong et al. 2003). These spontaneous mutations have been shown to have a high rate of reversion back to wild-type, however, and would not survive the multiple rounds of selection necessary for homing peptide isolation. Therefore, it would be desirable to design phage libraries that would have longer circulation times and retain this feature through the multiple rounds of *in vivo* selection. The T7 phage vector was mutated in both positions in gene 17 with four base pair substitutions to increase the half life of circulating, infectious phage and also decrease the chance of the phage reverting back to the wild-type phenotype.

The atherosclerotic plaque microenvironment shares several similarities to that of tumor tissue, such as hypoxia, inflammation, angiogenesis, and oxidative stresses. There is an increasing body of evidence that establishes several genetic and proteomic factors that are common to these diseases (Ross, Stagliano et al. 2001; Ramos and Partridge 2005; Jain, Finn et al. 2007). Due to the commonality between these diseases we hypothesized that some of the peptides that were discovered to target the vasculature of tumors *in vivo* would also bind to atherosclerotic lesions. *In vivo* phage display is a high throughput format that allows multiple peptides to be tested very quickly for binding to plaques. T7 phage also act as a prototypic nanoparticle due to its size and avidity. Therefore, peptides displayed on the surface of phage that cause binding to plaques should translate well over to other nanoparticles. Our work demonstrates that



the commonalities between tumors and plaques can be exploited in the design of targeting elements for these diseased tissues.

## Methods

**Mutagenesis of T7 phage tail proteins.** T7Select Phage DNA (1-1, 10-3b, and 415-1, Novagen, Gibbstown, NJ ) was isolated using the Qiagen Lambda Maxi Kit (Qiagen, Valencia, CA). The region of interest in gene 17 was amplified using PCR to avoid having to work with the full length vector which is around 30,000bp. PCR mutagenesis was performed in two steps. The first step used two PCR reactions, each one causing a mutation at a particular site. The second step amplified the two fragments together with ApaLI and BglI restriction sites to clone back into the phage vector (Figure 3.2). The PCR primers used in the reactions were: ApaLI-up (TACGCTCTGCCTAAGGAGAA), Right V/D mutation primer (CCGATCGGCTTCGTCTACGAAACCCTTG), Left V/D mutation primer (TTCGTAGACGAAGCCGATCGGTTCAAGA), and BglI-down (GTAGGTAAGCATCCAGCCAT). The PCR product from the second reaction and the cyclized phage vector DNA were then cut with ApaLI and BglI restriction enzymes and the mutated insert was ligated back into the phage vector arms. The product of the ligation reaction was packaged using T7Select Packaging Extracts (Novagen, Gibbstown, NJ), and amplified in *E. coli*. The cleared lysate was then titered, and individual clones were sequenced (207/211-Left-CCGTAATGAGGCTGAGACTT and

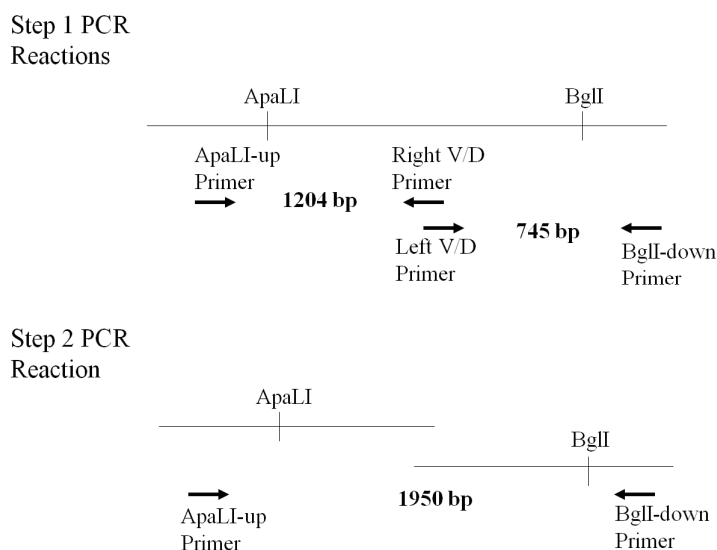


**Figure 3.2:** PCR mutagenesis of T7 phage vector. Mutagenesis was performed in two steps. In the first reaction the mutations were introduced into the DNA sequence and the ApaLI-up and right V/D primers produced a 1204bp product and the left V/D and BglI-down primers produced a 745bp product. In the second PCR reaction the full length mutated sequence was amplified using the ApaLI-up and BglI-down primers producing a 1950bp insert.

207/211-Right-GATGCTGTGGCAGAGTTCTC) to determine clones that contained both mutations in gene 17.

**Circulation time of mutated phage.** Mice were anesthetized for procedures with a ketamine-xylazine cocktail (80-100mg/kg and 5-10mg/kg, respectively) intraperitoneally and monitored using a toe pinch with more anesthetic given as needed. Mutated or wild-type insertless (do not contain a C-terminal fusion peptide) T7 phage clones ( $10^{10}$  pfu) were injected intravenously into the tail veins of C57BL/6J mice and allowed to circulate. Blood was drawn from the orbital sinus at various time points and 10 $\mu$ l of whole blood was diluted in serial dilutions to titer the circulating phage in the blood.

**Phage uptake by the liver.** Mutated or wild-type insertless (do not contain a C-terminal fusion peptide) T7 phage clones ( $10^{10}$  pfu) were injected intravenously into the tail veins of C57BL/6J mice and allowed to circulate. The mice were perfused with cold DMEM through the left ventricle and the liver was excised. Livers were weighed and then homogenized in cold DMEM. Homogenates were then washed in DMEM and titered for bound phage. Phage in the homogenates from mice injected with mutant phage were amplified with *E. coli* and injected intravenously into another mouse for the next round of selection. This process was repeated for 4 rounds of selection.

**Phage playoff screen for peptides that bind to atherosclerotic plaques.**

Oligonucleotides coding for CG7C (CGGGGGGGC), LyP-1 (CGNKRTRGC), a Metadherin fragment (GLNGLSSADPSSDWNAPAEWGNWVDEDRASLLKSQEPISNDQKVSDDDKEKGEGALPTGKSK), CRK (CRKDKC), CARS (CARSTAKTC), CSG (CAPGPSKSC), CLT-1 (CGLIIQKNEC), CLT-2 (CNAGESSKNC), CGKRK (CGKRK), and CREKA (CREKA) peptides were cloned into T7Select 415-1 (Novagen, Gibbstown, NJ) phage DNA vectors arms according to the established protocol from Novagen. Individual clones were mixed in equal ratios to make a pool of phage which was injected intravenously into ApoE knockout mice on a high fat diet for 6 months and allowed to circulate for 10 minutes. The mice were then perfused with 40ml of cold DMEM through the left ventricle to remove any unbound phage and the aortic tree was excised. Plaques could be visually seen in the upper region of the aorta and its three main branches. The tissue was washed and homogenized in cold DMEM. The homogenate was titered and individual clones were

sequenced to determine what insert they contained. The sequencing primers used were SuperUp-AGCGGACCAGATTATCGCTA and Down-AACCCCTCAAGACCCGTTTA. The ratio of the number of each phage in the output pool to the number of each phage in the input pool was plotted.

**Testing individual phage clones.** Confirmation of homing by the peptides in the phage pool was conducted by individually injecting each phage clone into ApoE mice fed a high fat diet. The phage were injected intravenously into the tail vein of mice and allowed to circulate for 10 minutes. Anesthetized mice were then perfused through the left ventricle with 40ml of cold DMEM to remove unbound phage and the aortic tree was excised. Tissue that contained atherosclerotic lesions was separated from healthy tissue. The tissue was washed in DMEM and then homogenized. Homogenized tissue was titered and the ratio of the phage bound to the atherosclerotic tissue to phage bound to healthy tissue was plotted for each phage clone.

## Results

**Long-circulating phage.** Two mutations were made in gene 17 that changed the arginine at position 207 to a valine and the lysine at position 211 to be an aspartate (Figure 3.3). These changes in the charges of the residues have been reported to disrupt the coiled-coil domain of the tail proteins (Sokoloff, Wong et al. 2003). Mutated phage or wild-type T7 phage were then injected into mice and blood was collected at various time points to determine the effect of the mutations on circulation time of the phage.

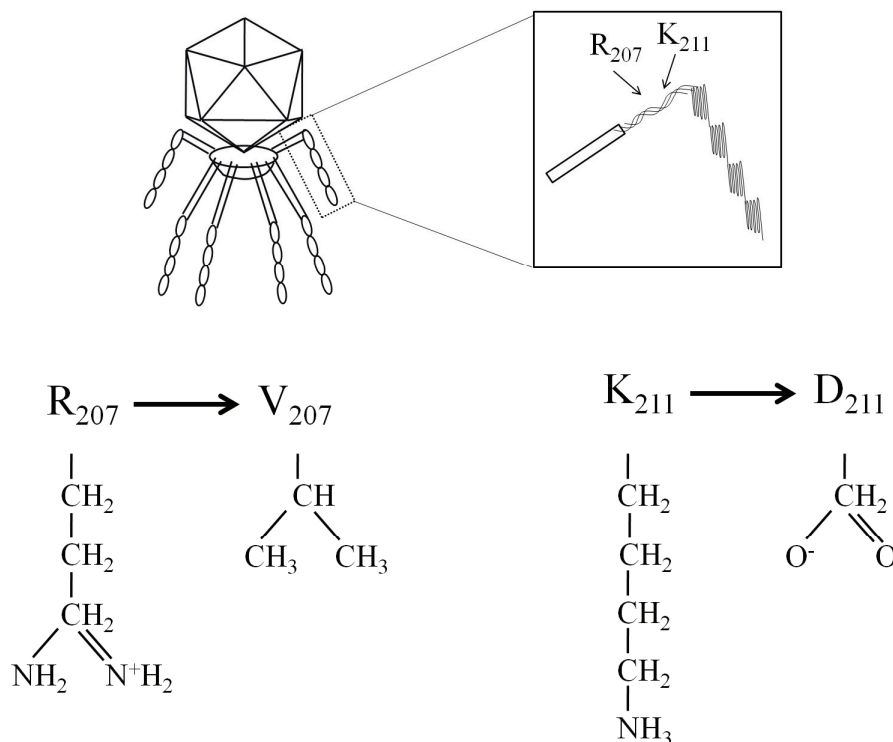


**Figure 3.3:** Mutations in the tail protein of long-circulating T7 phage. Two mutations were made in gene 17 of the phage, disrupting the coiled-coil structure of the tail proteins. The strong positive charge of the arginine residue at position 207 was converted to a neutral charge of a valine and the strong positive charge of the lysine at position 211 was changed to a negative charge of an aspartate residue.

The R207V/K211D mutations in the T7 phage tail proteins had a dramatic effect on circulation time as can be seen in Figure 3.4A. After 30 minutes of circulation, 70% of the mutant phage were still in the circulation and were infectious (able to be amplified). On the other hand, only 17% of the control, wild-type phage remained in circulation. Half-life for the mutated phage was determined to be 182 minutes compared to the half-life of 7 minutes seen in the wild-type phage. Lower titers were also seen in the livers of mice injected with mutant phage. This effect remained through multiple rounds of selection using liver tissue. Even after 4 rounds of selection with phage that did not contain a C-terminal fusion peptide, none mutated phage reverted

back to the wild-type phenotype. Also less than one-fifth as many of the mutated phage were taken into the liver compared to wild-type phage (Figure 3.4B). All of the mutated phage that were sequenced after the four rounds of selection contained had both of the mutations in gene 17.

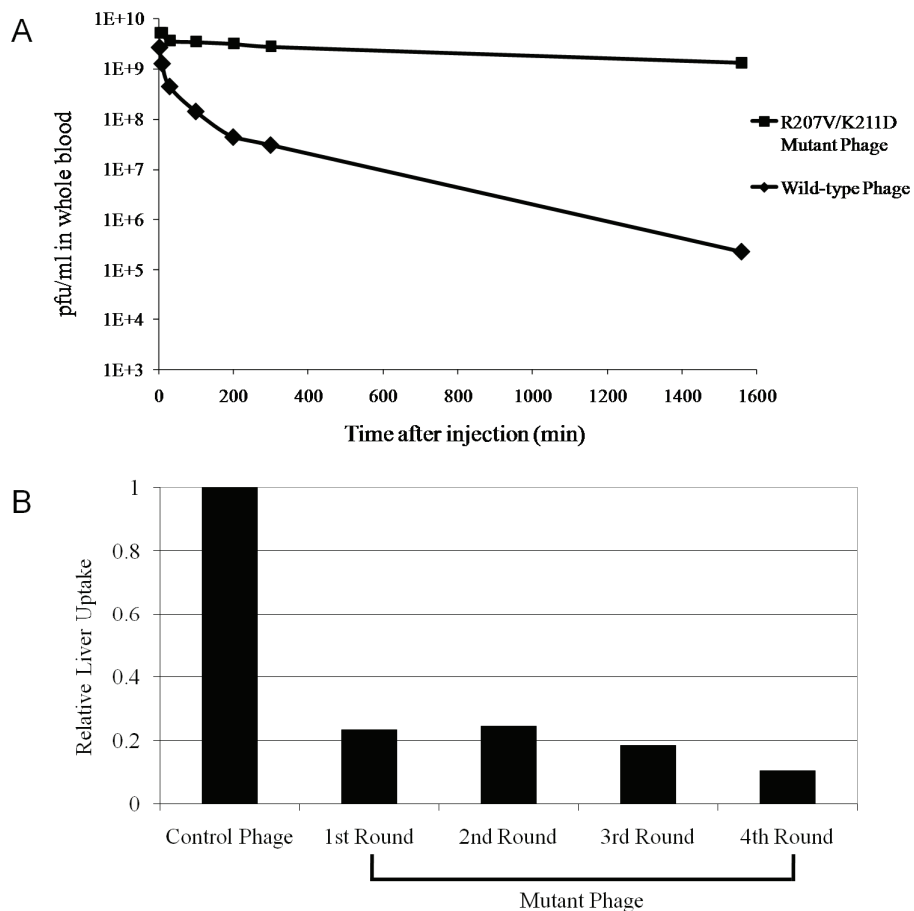


**Figure 3.4:** Tail mutations in T7 phage. (A) T7 phage with two amino acid substitutions in the tail fiber proteins have a much longer circulation time in the blood of mice than wild-type T7 phage (n=6 mice for R207V/K211D mutant phage and n=3 mice for wild-type phage). (B) Fewer phage are also found in the liver after 10 minutes of circulation with the mutated phage compared to the wild-type. After 4 rounds of selection mutated phage have still not reverted back to the wild-type phenotype and continue to have lower uptake into the liver.

***In vivo* phage screens for new plaque targeting peptides.** Sequences of peptides that target the vasculature of various tumors were cloned into T7 phage vectors so that around 200 copies were expressed as a C-terminal fusion to the capsid protein. Various phage clones that target tumor vasculature were mixed together in equal ratios to form a phage pool. Phage containing the insert coding for a cyclic glycine peptide (CG7C) served as an internal control. This phage pool was then injected into an ApoE null mouse that had been on a high fat diet for 6 months and allowed to circulate and bind. Phage containing inserts that code for the CLT-1, CLT-2, and CREKA peptides all had a much higher proportional representation of the phage that were eluted from the aortic tree where plaques were located (Figure 3.5). Individual phage clones were then

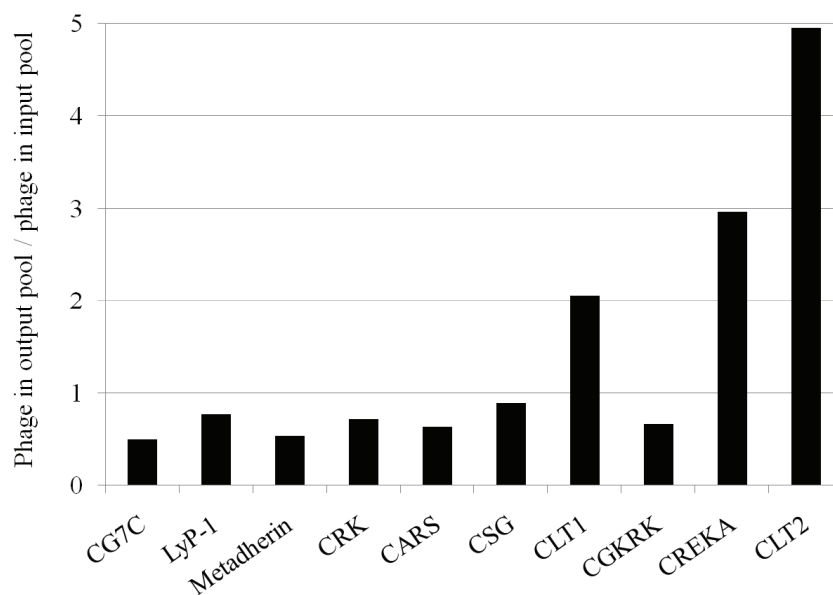


**Figure 3.5:** Phage playoff screen of known homing peptides for atherosclerotic plaques. Various phage clones expressing peptides that are known to target tumor blood vessels were pooled together and injected into an atherosclerotic, ApoE null mouse on a high fat diet. The aortic tree containing atherosclerotic plaques was isolated and the bound phage were eluted and sequenced. A cyclic glycine peptide (CG7C) served as a control.

injected into atherosclerotic, ApoE mice to confirm the results from the phage pool screen. Mice injected with CLT-1 expressing phage had 6.3 times more phage bound to regions that contained plaques than areas of the vasculature that were free of plaques. Mice injected with CLT-2 expressing phage had 6.1 times more phage bound to regions that contained plaques than areas of the vasculature that were free of plaques. CREKA expressing phage had an 8.7 times higher specificity for plaque-containing regions of the vasculature than healthy portions. Phage expressing CG7C did not have a higher specificity for diseased areas of the vessel compared to healthy (Figure 3.6). All of the phage clones had a similar number of phage that bound to the healthy portions of the vessel.

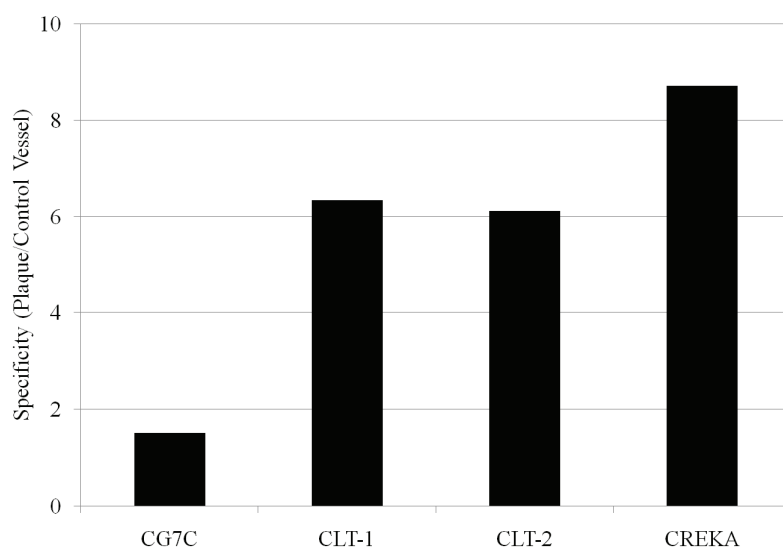


**Figure 3.6:** Phage homing to atherosclerotic plaques. Individual phage clones expressing various peptides that are known to target tumor blood vessels were individually injected into ApoE null mice on a high fat diet. The aortic tree containing atherosclerotic plaques and vessels that did not contain plaques were isolated. Bound phage were eluted and titered. The specificity of phage to target plaque tissue is plotted with the ratio of phage in vessels with plaques compared to phage in vessels clear of plaques for each phage clone. A cyclic glycine peptide (CG7C) served as the control.



## Discussion

*In vivo* phage display has been shown to be a very effective technique for isolating peptides that can differentiate and target the various vascular beds in the body, but the short half life of T7 phage in circulation, due to its rapid uptake by the liver, limits its usefulness in many screens. Mutations at either site in gene 17 disrupt the coiled-coil structure and decrease the uptake of the phage by hepatocytes in the liver (Sokoloff, Wong et al. 2003), but due to the high rate of mutation in phage, reversion to the wild-type phenotype occurs with high frequency after multiple rounds of amplification. Instead of making a single base pair mutation to induce one amino acid substitution, two base pairs were mutated at each site, giving a total of four mutations. These mutations greatly reduced the likelihood that the phage would revert back to the wild-type phenotype. The mutations were highly effective at increasing the phage circulation time and prevented reversion. Even after 4 rounds of selection for phage in the liver, all of the sequenced phage contained the mutations.

Longer circulating phage will have more time to reach their target, which could lead to more effective *in vivo* phage screens using T7 phage. Also screens that were not possible due to the high background of T7 phage found in the liver, due to nonspecific uptake, are possible with the mutated phage. One screen that is currently being conducted in our lab using these mutated phage is to find peptides that bind cells in the reticuloendothelial system (RES). Many types of nanoparticles including iron oxide particles are removed from the circulation very quickly. Various methods have been used to decrease the uptake by the RES, including injecting nickel liposomes (Simberg,

Duza et al. 2007), but finding peptides that bind to the RES and prevent uptake of the iron oxide particles might provide an effective approach to increase circulation time of iron oxide nanoparticles with less toxicity.

*In vivo* phage display was used to test known peptide sequences that target tumors for their ability to home to atherosclerotic plaques. Tumors and plaques share a similar microenvironment and therefore might contain similar markers on their cells that are available for targeting. Phage expressing CREKA, CLT-1, or CLT-2 peptides on their surface showed increased binding to the plaque tissue in the ApoE knockout mouse model of atherosclerosis. Increased binding was observed in both the playoff screen in which many phage clones were injected together and when these clones were tested individually. The binding also appeared to be specific because a higher ratio of these phage clones bound to the atherosclerotic regions of the vessel compared to the healthy portions. All three of these peptides have been shown to bind to clotted plasma proteins and colocalize with fibrin(ogen) present in the extravascular compartment of tumors (Pilch, Brown et al. 2006; Simberg, Duza et al. 2007). Subtle clotting in atherosclerotic plaques has been observed through deposition of fibrin/fibrinogen both inside and on the surface of atherosclerotic plaques (Duguid 1946; Duguid 1948; Smith 1993) making these peptides potentially valuable targeting elements for atherosclerotic plaques.

## References

- Duguid, J. B. (1946). "Thrombosis as a Factor in the Pathogenesis of Coronary Atherosclerosis." J Pathol Bacterial **58**(2): 207-212.
- Duguid, J. B. (1948). "Thrombosis as a factor in the pathogenesis of aortic atherosclerosis." J Pathol Bacterial **60**(1): 57-61.
- Fan, X., R. Venegas, R. Fey, H. van der Heyde, M. A. Bernard, E. Lazarides and C. M. Woods (2007). "An in vivo approach to structure activity relationship analysis of peptide ligands." Pharm Res **24**(5): 868-79.
- Hoffman, J. A., E. Giraudo, M. Singh, L. Zhang, M. Inoue, K. Porkka, D. Hanahan and E. Ruoslahti (2003). "Progressive vascular changes in a transgenic mouse model of squamous cell carcinoma." Cancer Cell **4**(5): 383-91.
- Jain, R. K., A. V. Finn, F. D. Kolodgie, H. K. Gold and R. Virmani (2007). "Antiangiogenic therapy for normalization of atherosclerotic plaque vasculature: a potential strategy for plaque stabilization." Nat Clin Pract Cardiovasc Med **4**(9): 491-502.
- Kehoe, J. W. and B. K. Kay (2005). "Filamentous phage display in the new millennium." Chem Rev **105**(11): 4056-72.
- Kelly, K. A., M. Nahrendorf, A. M. Yu, F. Reynolds and R. Weissleder (2006). "In vivo phage display selection yields atherosclerotic plaque targeted peptides for imaging." Mol Imaging Biol **8**(4): 201-7.
- Pasqualini, R. and E. Ruoslahti (1996). "Organ targeting in vivo using phage display peptide libraries." Nature **380**(6572): 364-6.
- Pilch, J., D. M. Brown, M. Komatsu, T. A. Jarvinen, M. Yang, D. Peters, R. M. Hoffman and E. Ruoslahti (2006). "Peptides selected for binding to clotted plasma accumulate in tumor stroma and wounds." Proc Natl Acad Sci U S A **103**(8): 2800-4.
- Ramos, K. S. and C. R. Partridge (2005). "Atherosclerosis and cancer: flip sides of the neoplastic response in mammalian cells?" Cardiovasc Toxicol **5**(3): 245-55.
- Rosenberg, A., K. Griffin, F. W. Studier, M. McCormick, J. Berg, R. Novy and R. Mierendorf (1996). "T7Select Phage Display System: A powerful new protein display system based on bacteriophage T7." inNovations **6**: 1-6.

- Ross, J. S., N. E. Stagliano, M. J. Donovan, R. E. Breitbart and G. S. Ginsburg (2001). "Atherosclerosis and cancer: common molecular pathways of disease development and progression." Ann N Y Acad Sci **947**: 271-92; discussion 292-3.
- Simberg, D., T. Duza, J. H. Park, M. Essler, J. Pilch, L. Zhang, A. M. Derfus, M. Yang, R. M. Hoffman, S. Bhatia, M. J. Sailor and E. Ruoslahti (2007). "Biomimetic amplification of nanoparticle homing to tumors." Proc Natl Acad Sci U S A **104**(3): 932-6.
- Smith, E. B. (1993). "Fibrinogen and atherosclerosis." Wien Klin Wochenschr **105**(15): 417-24.
- Smith, G. P. (1985). "Filamentous fusion phage: novel expression vectors that display cloned antigens on the virion surface." Science **228**(4705): 1315-7.
- Smith, G. P. and V. A. Petrenko (1997). "Phage Display." Chem Rev **97**(2): 391-410.
- Sokoloff, A. V., S. C. Wong, J. J. Ludtke, M. G. Sebestyen, V. M. Subbotin, G. Zhang, T. Budker, M. Bachhuber, Y. Sumita and J. A. Wolff (2003). "A new peptide ligand that targets particles and heterologous proteins to hepatocytes in vivo." Mol Ther **8**(6): 867-72.

## Chapter 4

### **Targeting atherosclerosis using CREKA targeted, modular, multifunctional micelles**

#### **Abstract**

Subtle clotting that occurs on the luminal surface of atherosclerotic plaques, presents a novel target for nanoparticle-based diagnostics and therapeutics. We have developed multifunctional, modular micelles that contain a targeting element, a fluorophore and, when desired, a drug component in the same particle. Targeting atherosclerotic plaques in ApoE null mice fed a high fat diet was accomplished with the pentapeptide CREKA (cysteine-arginine-glutamic acid-lysine-alanine), which binds to clotted plasma proteins. The fluorescent micelles bind to the entire surface of the plaque and notably, concentrate at the shoulders of the plaque, a location that is prone to rupture. We also show that the targeted micelles deliver an increased concentration of the anticoagulant drug, hirulog, to the plaque when compared to untargeted micelles.

#### **Introduction**

Cardiovascular disease affects 1 in 3 people in the United States during their lifetime and accounts for nearly a third of the deaths that occur each year (Rosamond, Flegal et al. 2007). Atherosclerosis is one of the leading causes of cardiovascular

disease and results in raised plaques in the arterial wall that can occlude the vascular lumen and block blood flow through the vessel. Recently, it has become clear that not all plaques are the same: those susceptible to rupture, fissuring, and subsequent thrombosis are most frequently the cause of acute coronary syndromes and death (Davies 1992).

Rupture of an atherosclerotic plaque exposes collagen and other plaque components to the bloodstream. This initiates hemostasis in the blood vessel and leads to activation of thrombin and a thrombus to form at the site of rupture. Elevated levels of activated thrombin bound to the vessel wall have been observed up to 72 hours after vascular injury (Ghigliotti, Waissbluth et al. 1998). These elevated thrombin levels not only induce clot formation but also have been implicated in the progression of atherosclerosis by causing smooth muscle cells to bind circulating low density lipoprotein (Ivey and Little 2008). Subtle clotting in plaques is also indicated by deposition of fibrin/fibrinogen both inside and on the surface of atherosclerotic plaques, which has been well documented since the 1940's (Duguid 1946; Duguid 1948; Smith 1993).

Fibrin-containing blood clots have been extensively used as a target for site-specific delivery of imaging agents and anti-clotting agents to thrombi (Bode, Hudelmayer et al. 1994; Alonso, Della Martina et al. 2007; Stoll, Bassler et al. 2007). Delivering anticoagulants into vessels where clotting is taking place has been shown to be effective at reducing the formation and expansion of clots and also decreases the risk of systemic side effects (Bode, Hudelmayer et al. 1994; Stoll, Bassler et al. 2007).

Antibodies and peptides that bind to molecular markers specifically expressed on atherosclerotic plaques have shown promise for plaque imaging *in vivo* (Houston, Goodman et al. 2001; Liu, Bhattacharjee et al. 2003; Kelly, Nahrendorf et al. 2006; Briley-Saebo, Shaw et al. 2008), but clotting on the plaque has not been used as a target. We reasoned that the fibrin deposited on plaques could serve as a target for delivering diagnostic and therapeutic compounds to plaques.

We chose the clot-binding peptide CREKA to test the suitability of fibrin(ogen) (clotted plasma proteins) for plaque targeting. This peptide was identified as a tumor-homing peptide by *in vivo* phage library screening (Fig 4.1) and subsequently shown to bind to clotted plasma proteins in the blood vessels and stroma of tumors (Simberg, Duza et al. 2007; Karmali, Kotamraju et al. 2008). Here we show that CREKA-targeted micelles can be used to deliver and concentrate imaging dyes and the direct thrombin inhibitor, hirulog in atherosclerotic plaques in the ApoE null mouse model *in vivo*.

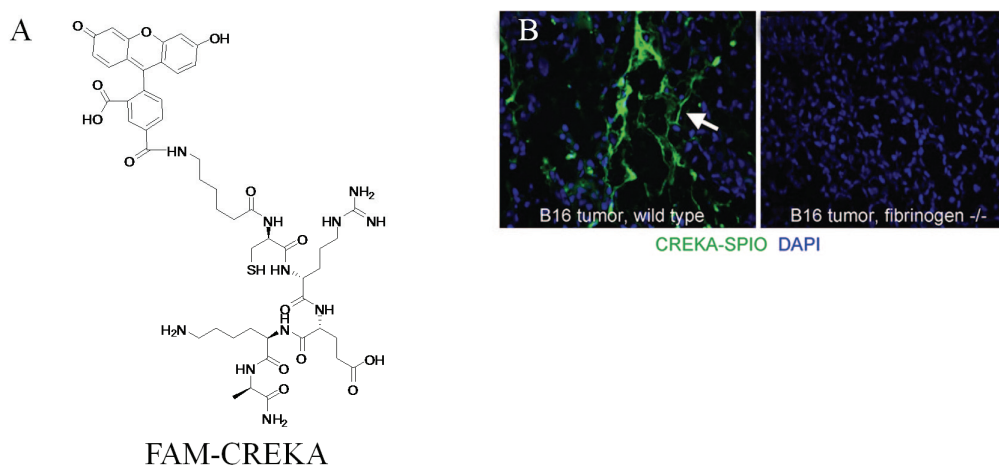


**Figure 4.1:** Structure and homing of carboxyfluorescein (FAM)-CREKA penta-peptide. (A) Chemical structure of FAM-CREKA. (B) FAM-CREKA bound to the blood vessels and stroma of B16F1 melanoma tumors in wild-type mice but not mice that lack fibrinogen (Figure 1B is reproduced with permission from Simberg et al. 2007).

## Materials and Methods

**Micelles.** The anticoagulant peptide hirulog-2 was modified by adding a cysteine residue to the N-terminus (Cys-(D-Phe)-Pro-Arg-Pro-(Gly)<sub>4</sub>-Asn-Gly-Asp-Phe-Glu-Glu-Ile-Pro-Glu-Glu-Tyr-Leu) for covalent conjugation to the micelle lipid tail. Synthesis of all of the peptides was performed by adapting Fmoc/t-Bu strategy on a microwave assisted automated peptide synthesizer (Liberty, CEM Corporation). Peptide crudes were purified by HPLC using 0.1% TFA in acetonitrile-water mixtures. The peptides obtained were 90% - 95% pure by HPLC and were characterized by Q-TOF mass spectral analysis.

1,2-distearoyl-sn-glycero-3-phosphoethanolamine-N-[maleimide(polyethylene glycol)-2000] (DSPE-PEG(2000)-maleimide) and 1,2-distearoyl-sn-glycero-3-phosphoethanolamine-N-[amino(polyethylene glycol)-2000] (DSPE-PEG(2000)-amine) were purchased from Avanti Polar Lipids, Inc. Cy7 mono NHS ester was purchased from Amersham Biosciences.

Cysteine-containing peptides were conjugated via a thioether linkage to DSPE-PEG(2000)-maleimide by adding a 10% molar excess of the lipid to a water : methanol solution (90:10 by volume) containing the peptide. After reaction at room temperature for 4 hours, a solution of N-acetyl cysteine (Sigma) was added to react with free maleimide groups. The resulting product was then purified by reverse-phase, high-performance, liquid-chromatography (HPLC) on a C4 column (Vydac) at 60°C.

Cy7 was conjugated via a peptide bond to DSPE-PEG(2000)-amine by adding a 3-fold molar excess of Cy7 mono NHS ester to the lipid dissolved in 10mM aqueous



carbonate buffer (pH = 8.5) containing 10% methanol by volume. After reaction at 4°C for 8 hours, the mixture was purified by HPLC as above.

Mixtures of fluorophore and peptide-containing DSPE-PEG(2000) amphiphiles were prepared in a glass culture tube by dissolving each pure component in methanol, mixing the components, and evaporating the mixed solution under nitrogen. The resulting film was dried under vacuum for 8 hours then hydrated at 80°C in water with a salt concentration of 10mM NaCl. Samples were incubated at 80°C for 30 minutes and allowed to cool to room temperature for 60 minutes. Solutions were then filtered through a 220nm poly(vinylidene fluoride) syringe filter (Fisher Scientific).

**Micelle Size as Determined by Dynamic Light Scattering.** The presence of small, spheroidal micelles was confirmed by particle size measurements using dynamic light scattering (DLS). The DLS system (Brookhaven Instruments) consisted of an avalanche photodiode detector to measure scattering intensity from a 632.8nm HeNe laser (Melles Griot) as a function of delay time. A goniometer was used to vary measurement angle, and consequently, the scattering wave vector,  $q$ .

The first cumulant,  $\Gamma$ , of the first-order autocorrelation function was measured as a function of scattering wave vector in the range 0.015 to 0.025nm<sup>-1</sup>. The quantity,  $\Gamma/q^2$ , was linearly extrapolated to  $q = 0$  to determine the translational diffusion coefficient of the aggregate and the Stokes-Einstein [perhaps a reference for the less physical science inclined] relationship was used to estimate the micelle hydrodynamic diameter based on the measured diffusion coefficient.

**Half-life of Micelles in Circulation.** The half-life of FAM-CREKA micelles in circulation was determined by injecting 100 $\mu$ L of 1mM solution of micelles into Balb/c wild-type mice intravenously. Blood was collected from the retro-orbital sinus with heparinized capillary tubes from the same mouse at various time points post injection. The blood was centrifuged at 1000g for 2 min, and a 10 $\mu$ L aliquot of plasma was diluted to 100 $\mu$ L with PBS. Fluorescence of the plasma was measured using a fluorimeter at an excitation wavelength of 485nm and emission wavelength of 528nm.

The half-life of FAM-CREKA/Cy7/hirulog mixed micelles in circulation was determined by injecting 100 $\mu$ l of 1mM micelles into C57BL/6 wild-type mice intravenously. Blood was collected in 3.2% buffered sodium citrate at various time points from different mice by cardiac puncture and centrifuged at 1000g for 10min. Plasma was then analyzed for anti-thrombin activity using an assay with the S-2366 chromogenic substrate according to the published protocol for hirudin (Fig 4.2, diaPharma, West Chester, Ohio).

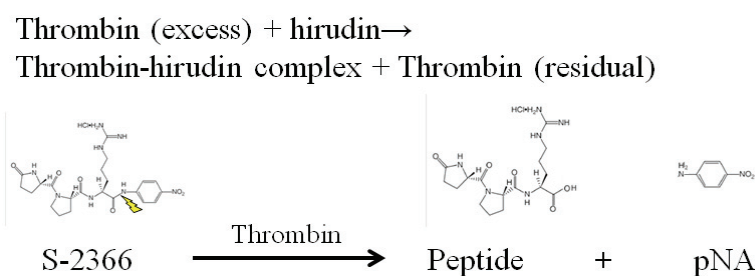


**Figure 4.2:** Thrombin activity chromogenic assay. Excess thrombin was incubated with the sample containing hirudin and allowed to complex. Residual thrombin cleaves the chromogenic substrate S-2366 into a peptide and free p-nitroaniline (pNA) which absorbs light at 405nm.

**Targeting of Micelles to Atherosclerotic Plaques.** Transgenic mice homozygous for the Apoe<sup>tm1Unc</sup> mutation (Jackson labs, Bar Harbor, ME) were fed a high fat diet (42% fat, TD88137, Harlan, Madison, WI) for 6 months to generate stage V lesions (Whitman 2004) in the brachiocephalic artery and aortic arch. Mice were housed and all procedures were performed according to standards of the University of California, Santa Barbara Institutional Animal Care and Use Committee. The mice were injected intravenously through the tail vein with 100 $\mu$ l, 1mM micelles containing either FAM-CREKA or a 1:1 mix of FAM and N-acetyl cysteine as head groups. Micelles were allowed to circulate in the mice for 3 hours and the mice were then perfused with ice cold Dulbecco's Modified Eagle Medium (DMEM) through the left ventricle to remove any unbound micelles. The heart, aortic tree, liver, spleen, lungs, and kidneys were excised and fixed with 4% paraformaldehyde overnight at 4°C. *Ex vivo* imaging was performed using a 530nm viewing filter, illuminator light source (Light Tools Research, Encinitas, CA) and a Canon XTi DSLR camera. Tissue was then treated with a 30% sucrose solution for 8 hours and frozen in OCT for cryosectioning. Quantification of fluorescence intensity was performed using Image J software.

**Tumor Targeting with CREKA Micelles.** Orthotopic prostate cancer xenografts were generated by implanting 22Rv-1 ( $2 \times 10^6$  cells in 30 $\mu$ l of PBS) human prostate cancer cells, into the prostate gland of male nude mice. When tumor volumes reached approximately 500mm<sup>3</sup>, the mice were injected with 100 $\mu$ l of 1mM FAM-

CREKA micelles intravenously through the tail vein. The micelles were allowed to circulate for 3 hours and then mice were perfused through the left ventricle with ice cold DMEM. The tumor was excised and frozen in OCT for sectioning.

**Immunofluorescence.** Serial cross-sections 5 $\mu$ m thick of the brachiocephalic artery, aortic arch, healthy vessel, control organs, or 22Rv-1 prostate tumor were mounted on silane treated microscope slides (Scientific Device Laboratory, Des Plaines, IL) and allowed to air dry. Sections were fixed in ice-cold acetone for 5 minutes and then blocked with Image-iT FX signal enhancer (Invitrogen, Carlsbad, CA). Alexa Fluor 647 conjugated rat anti-mouse antibodies to CD31 and CD68 (AbD Serotech, Raleigh, NC) were used to visualize endothelial cells and macrophages and other lymphocytes, respectively. Fibrinogen was stained with a primary polyclonal antibody made in goat and Alexa Fluor 647 conjugated anti-goat secondary antibody (Invitrogen, Carlsbad, CA). Sections were co-stained with DAPI in ProLong Gold antifade mounting medium (Invitrogen, Carlsbad, CA). Images of the vessels were taken using a confocal microscope.

**Quantification of Hirulog Activity at Plaque Surface.** The mice were injected intravenously through the tail vein with 100 $\mu$ l, 1mM (total lipid content) mixed micelles containing FAM-CREKA, CREKA, Cy7, and hirulog as head groups in a 3:3:0.3:3.7 ratio, respectively. Micelles were allowed to circulate in the mice for 3 hours and then mice were perfused with ice cold DMEM through the left ventricle to

remove any unbound micelles. The aortic tree was excised and homogenized in 1ml of normal human plasma with sodium citrate (US Biological, Swampscott, MA). Hirulog anti-thrombin activity was then quantified using an assay with the S-2366 chromogenic substrate according to the published protocol for hirudin (diaPharma, West Chester, Ohio).

**CREKA homing after hirulog therapy.** ApoE knockout mice on a high fat diet for 6 months were injected intravenously every 12 hours with hirulog micelles (100 $\mu$ l of 1mM solution) for 72 hours. 2 hours after the last injection of hirulog, either CREKA-targeted or non-targeted micelles (100 $\mu$ l of 1mM solution) were injected intravenously into the mice. Micelles were allowed to circulate for 3 hours and the mice were then perfused with ice cold Dulbecco's Modified Eagle Medium (DMEM) through the left ventricle to remove any unbound micelles. The aortic tree was excised and fixed with 4% paraformaldehyde overnight at 4°C and *ex vivo* imaging was performed.

## Results

**Modular, Multifunctional Micelles.** The general structure of the micelles is shown in Figure 4.3. We designed individual lipopeptide monomers with a 1,2-distearoyl-sn-glycero-3-phosphoethanol-amine (DSPE) tail, a PEG(2000) spacer, and a variable head group, which was either the carboxyfluorescein (FAM)-CREKA peptide, an infrared

fluorophore, or the hirulog peptide. When placed in aqueous solution, these compounds formed micelles with an average hydrodynamic diameter of  $17.0 \pm 1.0$  nm. We made targeted micelles from the FAM-CREKA monomers alone, or by mixing all three monomers together. Non-targeted control micelles were obtained by mixing FAM-

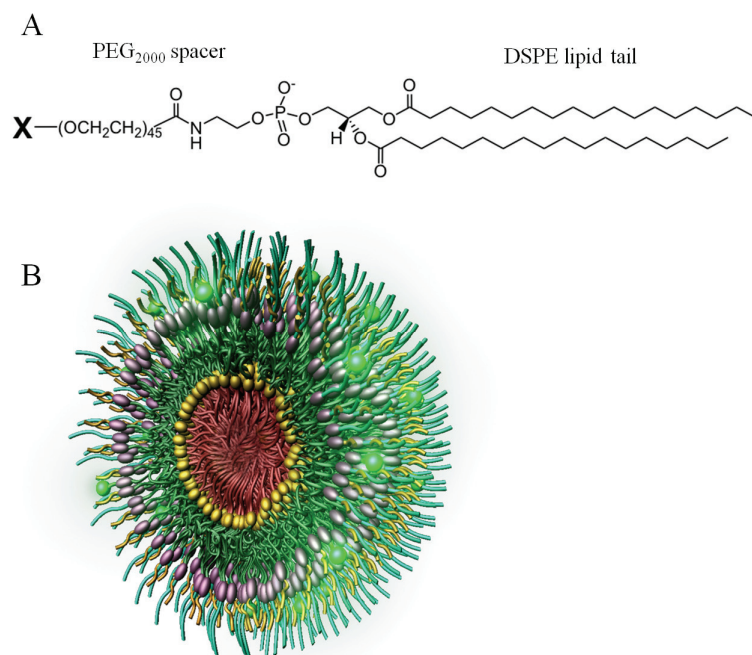


**Figure 4.3:** Construction of modular, multifunctional micelles. (A) Individual lipopeptide monomers are made up of a 1,2-distearoyl-sn-glycero-3-phosphoethanol-amine (DSPE) tail, a polyethyleneglycol (PEG2000) spacer, and a variable polar headgroup that contains either CREKA, FAM-CREKA, FAM, N-acetyl-cysteine, Cy7, or hirulog. The monomers were combined to form various mixed micelles. (B) Three dimensional rendering of FAM-CREKA/Cy7/hirulog mixed micelle.

labeled monomers with N-acetyl cysteine monomers. Half-life of FAM-CREKA micelles in circulation was determined by fluorescence and was 130 minutes. The half-life in circulation of the fluorescent CREKA/hirulog mixed micelles was determined using anti-thrombin activity and found to be about 90 minutes.

***Ex vivo* Imaging of the Aortic Tree in Atherosclerotic Mice.** We induced atherosclerotic plaques in ApoE null mice by keeping them on a high fat diet

(Nakashima, Plump et al. 1994; Reddick, Zhang et al. 1994). Earlier studies have revealed fibrin accumulation at the surface and interior of atherosclerotic plaques in other animal models and on human plaques (Eitzman, Westrick et al. 2000). We obtained similar results in the ApoE model; anti-fibrin(ogen) antibodies stained the plaques, but not normal-appearing vessel wall in this model (see Fig. 4.6A below), indicating the presence of clotted plasma proteins at these sites. To determine whether these fibrin deposits could serve as a target for imaging, we injected fluorescein-labeled CREKA micelles into these mice and imaged the isolated aortic tree *ex vivo*. High fluorescence intensity was observed in the regions that contained most of the atherosclerotic lesions. In the ApoE null mouse these regions include the brachiocephalic artery and the lower aortic arch (Maeda, Johnson et al. 2007). Quantitative comparison with fluorescent, non-targeted micelles revealed a large difference between the micelles that were targeted (fluorescence intensity in arbitrary units:  $277,000 \pm 10,000$ ) and those not targeted ( $5,100 \pm 3,300$ ; Fig 4.4). The difference was statistically significant ( $p \leq 0.001$ ). The fluorescence in the aortic tree from the CREKA-targeted micelles was abolished when an excess of unlabeled CREKA micelles was pre-injected ( $5,200 \pm 5,000$ ;  $p \leq 0.001$ ), whereas unlabeled, non-targeted micelles did not significantly inhibit the CREKA micelle homing ( $186,000 \pm 56,000$ ). These results indicate that CREKA micelles are able to specifically target the diseased vasculature in atherosclerotic mice and concentrate in areas that are prone to atherosclerotic plaque formation.

### Binding of CREKA Micelles to Atherosclerotic Plaques. Histological

examination of the vascular tree from mice injected with CREKA micelles revealed fluorescence on the luminal surface of plaques, while there was no significant binding to the histologically healthy portion of the blood vessel in microscopic cross-sections (Fig 4.5). Strikingly, the micelles appeared to concentrate in the shoulder regions of the plaque where plaques are known to be prone to rupture (Richardson, Davies et al. 1989; Falk, Schwartz et al. 2007). Fluorescence from the micelles was seen underneath the

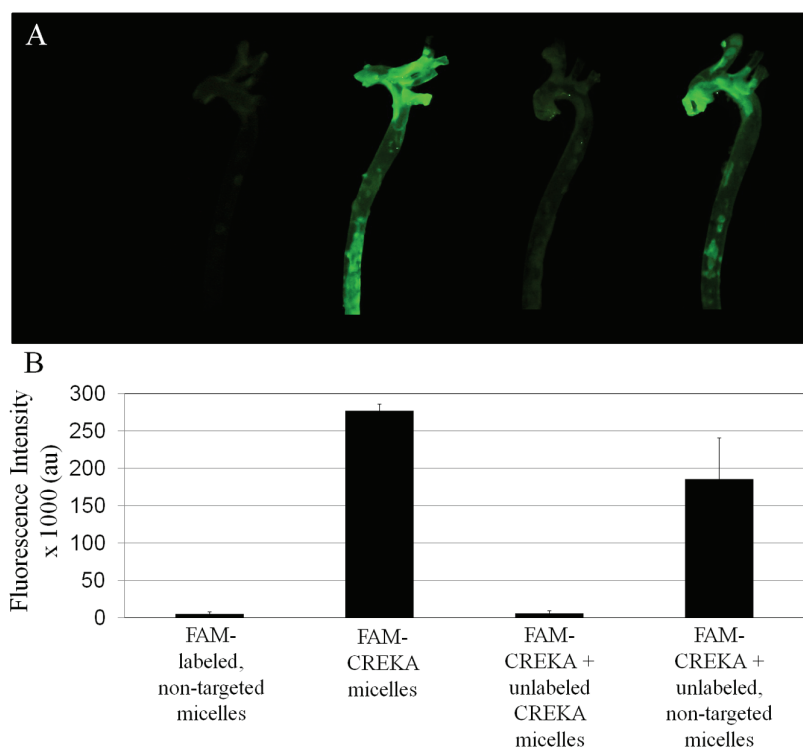


**Figure 4.4:** *Ex vivo* imaging of the aortic tree of atherosclerotic mice. Micelles were injected intravenously and allowed to circulate for three hours. The aortic tree was excised following perfusion and imaged *ex vivo*. (A) Increased fluorescence was observed in the aortic tree of ApoE null mice following injection with FAM-CREKA targeted micelles but not with non-targeted fluorescent micelles. When an excess of unlabeled CREKA micelles was injected prior to the FAM-CREKA micelles, fluorescence in the aortic tree was decreased. A pre-injection of an excess of non-targeted, unlabeled micelles did not cause a significant decrease in fluorescence. (B) Fluorescence in the aortic tree was quantified by measuring the intensity of fluorescent pixels (n=3 per group).



endothelial layer in the plaque in areas of high inflammation as shown with anti-CD31 (endothelial cells) and anti-CD68 (macrophages and lymphocytes) immunofluorescence (Figure 4.6A). Clotted plasma proteins were visualized on the surface of and throughout the interior of the plaque using anti-fibrinogen antibodies. CREKA micelles did not bind substantially to other tissues including the heart and lungs, but small quantities were found in the liver, spleen, and kidneys, tissues known to non-specifically trap nanoparticles (Fig 4.6B). Also, there was no accumulation of CREKA micelles in the aortas of normal mice (Fig 4.7). Thus, CREKA micelles specifically target atherosclerotic plaques, concentrating in areas that are prone to rupture with no appreciable binding to healthy vasculature.

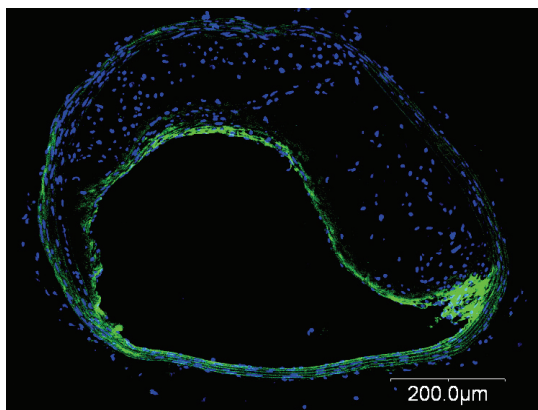


**Figure 4.5:** Binding of FAM-CREKA micelles to atherosclerotic plaque. ApoE null mice were injected with FAM-CREKA micelles which were allowed to circulate for 3 hours. Mice were perfused to remove unbound micelles and tissue cross-sections of the brachiocephalic artery (5 μm sections) were analyzed with a confocal microscope to determine binding. FAM-CREKA micelles appeared to bind to the entire surface of the atherosclerotic plaque, with no significant binding to the healthy portion of the vessel. Micelles appear to concentrate at the shoulder of the plaque (the portion where the healthy vessel and plaque meet) where most ruptures occur.

### **Role of Clotting in Binding of CREKA Micelles to Atherosclerotic Plaques.**

Binding of CREKA iron oxide nanoparticles to tumor vessels has previously been

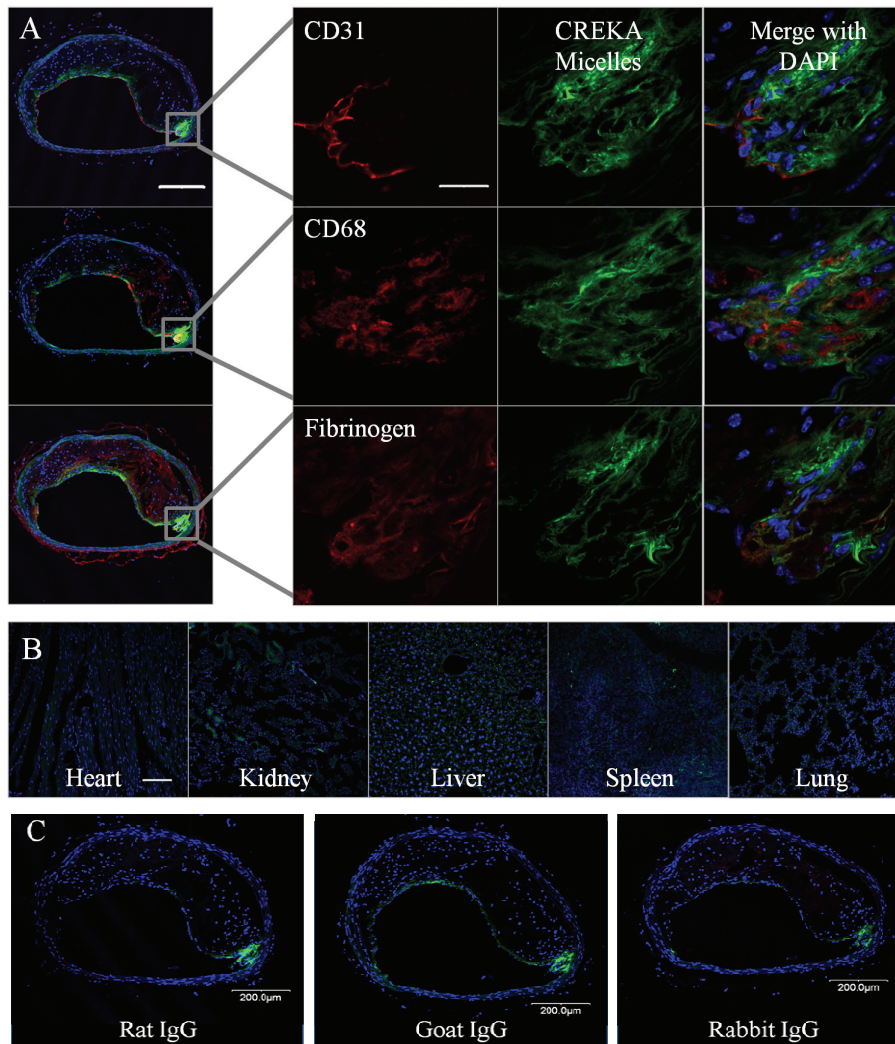


**Figure 4.6:** Localization of CREKA micelles in atherosclerotic plaques. (A) Serial cross-sections (5 $\mu$ m thick) were stained with antibodies against CD31 (endothelial cells), CD68 (macrophages and other lymphocytes), and fibrinogen. Representative microscopic fields are shown to illustrate the localization of micelle nanoparticles in the atherosclerotic plaque. Micelles are bound to the entire surface of the plaque with no apparent binding to the healthy portion of the vessel. CREKA targeted micelles also penetrate under the endothelial layer (CD31 staining) in the shoulder of the plaque (inset) where there is high inflammation (CD68 staining) and the plaque is prone to rupture. Clotted plasma proteins are seen throughout the plaque and its surface (fibrinogen staining). Images in the left panels were taken at a 10X magnification (bar=200 $\mu$ m) and images in the right panel are taken at a 150X magnification (bar=20 $\mu$ m). (B) Fluorescence was not observed in the heart or lung, and only a small amount was seen in the kidney, spleen, and liver. Images were taken at a 20X magnification (bar=100 $\mu$ m). (C) Negative controls for immunofluorescence.

injecting heparin, which prevented the clotting-induced amplification. The clotting-mediated amplification, while potentially beneficial in the diagnosis and treatment of cancer, would not be desirable in the management of atherosclerosis. No clotting was observed in the lumen of atherosclerotic blood vessels in microscopic cross-sections following injection of CREKA micelles. Furthermore, high fluorescence intensity was still observed in the aortas of atherosclerotic mice injected with FAM-CREKA micelles after a pre-injection of heparin (Fig 4.8A). In order to determine if the absence of

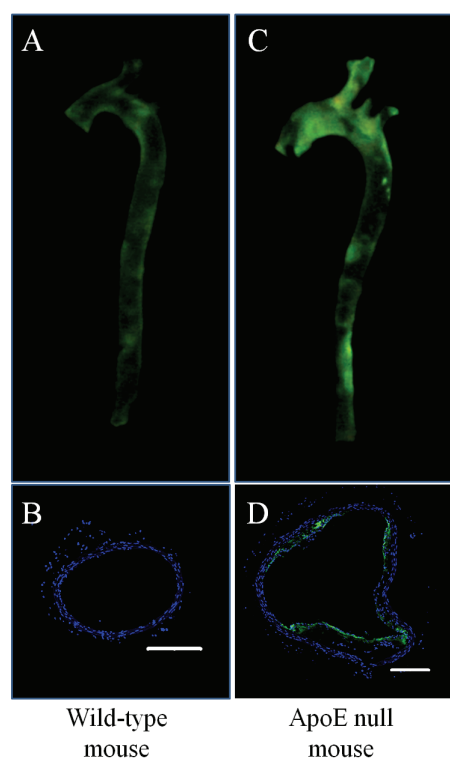


**Figure 4.7:** Targeting micelles to atherosclerotic plaques. ApoE null and wild-type mice were injected intravenously with FAM-CREKA micelles, which were allowed to circulate for 3 hours. (A, C) The aortic tree was excised following perfusion and imaged *ex vivo*. (B, D) Histological cross-sections were also analyzed for binding of micelles to the vessel wall. Higher fluorescence intensity was observed in (C) ApoE mice relative to (A) wild-type mice with *ex vivo* imaging. Fluorescent CREKA micelles did not bind to the healthy vessels in the histological sections of (B) wild-type mice but were observed on the surface of the atherosclerotic lesions in the (D) ApoE null mice. Histological images were taken at 10X magnification (bar=200 $\mu$ m).

induction of clotting by CREKA at the plaque surface was a characteristic of the micelles or the plaque microenvironment, we injected CREKA micelles into mice bearing 22RV1 tumors in which CREKA iron oxide nanoparticles cause intravascular clotting (L. Agemy and E. Ruoslahti, unpublished results). CREKA micelles accumulated at the walls of tumor vessels, but caused no detectable intravascular clotting (Fig 4.8B). Thus, unlike CREKA iron oxide particles (1), CREKA micelles do not seem to induce clotting in the target vessels, suggesting that the CREKA micellar platform is suitable for nanoparticle targeting to atherosclerotic plaques.

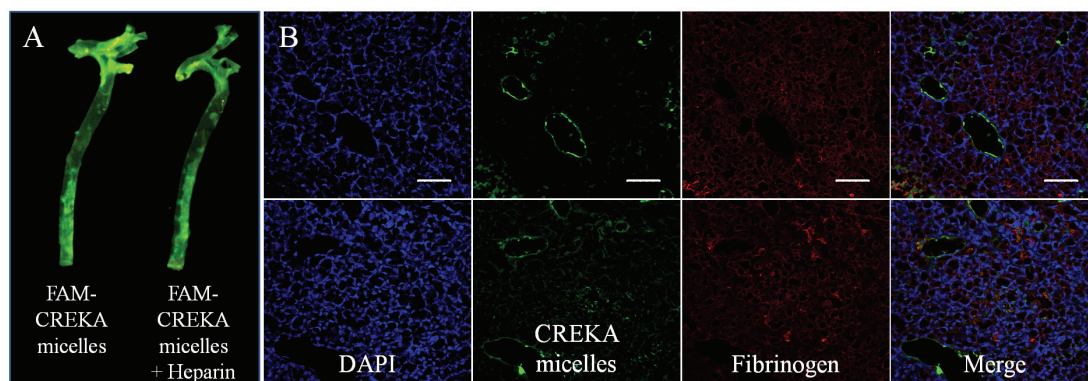


**Figure 4.8:** Role of clotting in binding of CREKA micelles. (A) Mice were injected intravenously with PBS or a bolus of 800 units/kg of heparin, followed 60 minutes later by 100 $\mu$ l of 1mM FAM-CREKA micelles. The mice received additional heparin (a total of 1,000 units/kg) or PBS throughout the experiment. Similar fluorescence was observed in the aortic tree of ApoE null mice that received a pre-injection of PBS or heparin followed by an injection of FAM-CREKA micelles. (B) CREKA micelles did not induce clotting in 22RV1 mouse prostate tumor model. Sections 5 $\mu$ m thick were stained with antibodies against fibrinogen. Representative microscopic fields are shown to illustrate that FAM-CREKA micelles bind to the blood vessels in the tumor but do not cause fibrin clots to form. Images were taken at 40X magnification (bar=50 $\mu$ m).

### Targeting of the Anti-Thrombin Peptide, Hirulog to Atherosclerotic

**Plaques.** The anticoagulant, heparin, is used in patients with unstable angina to prevent further clots from forming. However, this drug inhibits thrombin indirectly and cannot inhibit the thrombin that is already bound to fibrin. Moreover, its use can also lead to

serious complications including major bleeding events and thrombocytopenia. Direct thrombin inhibitors have fewer side effects and can inhibit thrombin that is already bound to a blood clot. Hirulog is a small synthetic peptide that was designed by combining the active sites from the natural thrombin inhibitor, hirudin, through a

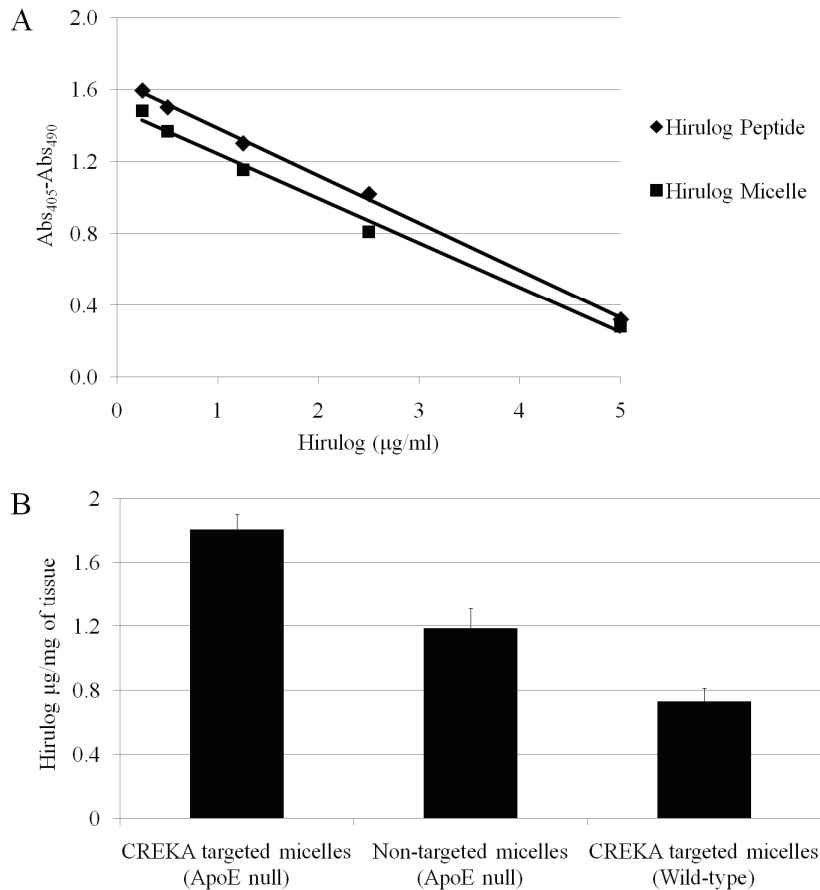


**Figure 4.9:** Targeting of hirulog to atherosclerotic plaques. (A) Equal molar concentrations of hirulog peptide and hirulog micelles were tested for anti-thrombin activity to ensure that potency did not decrease when hirulog was in micellar form. Hirulog peptide and micelles showed similar activity in a chromogenic assay. (B) CREKA targeted or non-targeted, hirulog mixed micelles were injected intravenously into mice and allowed to circulate for 3 hours. The aortic tree was excised and analyzed for bound hirulog. Significantly higher levels of anti-thrombin activity were observed in the aortic tree of ApoE null mice following injection of CREKA targeted hirulog micelles than non-targeted micelles (1.8µg/mg and 1.2µg/mg of tissue,  $p \leq 0.05$ ,  $n=3$  per group). Anti-thrombin activity generated by CREKA targeted hirulog micelles in ApoE null mice was also significantly higher than that in wild-type mice (0.8µg/mg of tissue,  $p \leq 0.05$ ,  $n=3$  per group).

flexible glycine linker into a single 20-amino acid peptide (Maraganore, Bourdon et al. 1990). We conjugated this peptide onto our micellar nanoparticles and showed that it retains full activity in a chromogenic assay for thrombin activity (Fig 4.9A). We next sought to use CREKA-targeted micelles to deliver hirulog to atherosclerotic plaques. CREKA/FAM/hirulog mixed micelles were injected into atherosclerotic mice and allowed to circulate for 3 hours. The accumulation of fluorescence in atherosclerotic aortas was identical to that of CREKA/FAM micelles described above (not shown). Anti-thrombin activity in the excised aortic tree was significantly higher in the aortas of mice injected with CREKA targeted micelles than in mice that received non-targeted micelles (1.8 $\mu$ g/mg and 1.2 $\mu$ g/mg of tissue,  $p \leq 0.05$ ). CREKA targeted micelles also caused significantly higher anti-thrombin activity in the aortas of atherosclerotic than wild type mice (0.8 $\mu$ g/mg of tissue,  $p \leq 0.05$ , Fig 4.9B). Thus, CREKA targeted micelles seem to selectively deliver hirulog to plaques.

Do to the fact that most patients are on anticoagulant therapy for long periods of time in the hospital, we wanted to see the effects of longer exposure to hirulog micelles and whether this affected CREKA homing. After 72 hours of intravenously injected high dose hirulog micelles (100 $\mu$ l of 1mM hirulog micelles), fluorescence was still observed with *ex vivo* imaging (Figure 4.10). Therefore, CREKA targeted micelles are still effective means of delivery for imaging agents and therapeutics even after long term anticoagulant therapy.

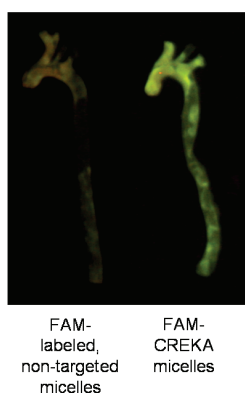


**Figure 4.10:** CREKA micelle homing after hirulog anticoagulant therapy. ApoE knockout mice on a high fat diet for 6 months were injected intravenously every 12 hours with 100 $\mu$ l, 1mM hirulog micelles for 72 hours. Either non-targeted or CREKA targeted micelles injected into mice and the aortic tree was imaged after 3 hours. Fluorescence was still visible in mice injected with CREKA targeted micelles even after 72 hours of hirulog anticoagulant therapy.

## Discussion

We describe the use of targeted micellar nanoparticles to direct both diagnostic imaging dyes and a therapeutic compound to atherosclerotic plaques *in vivo*. Mixed micelles composed of lipid-tailed clot-binding peptide CREKA as a targeting element, a fluorescent dye as a labeling agent and, in some cases, hirulog as an anticoagulant, specifically bound to plaques. The plaques accumulated fluorescence and, when hirulog was included in the micelles, an increased level of anti-thrombin activity was seen in the diseased vessels. The modularity that is inherent to our micellar nanoparticle platform allows multiple functions to be built into the nanoparticle.

Micelles coated with the CREKA peptide were able to specifically target diseased vasculature in ApoE null mice. The specificity of the targeting was evident from a number of observations: First, fluorescence from the micelles in the aortic tree of

atherosclerotic mice localized to known areas of plaque formation and no fluorescence was observed in wild-type mice. Second, CREKA micelles bind to the entire surface of the plaque in histological sections, but do not bind to the healthy portion of the vessel. Third, an excess of unlabeled CREKA micelles inhibited the plaque binding of fluorescent CREKA micelles. Thus, micelles targeted with the CREKA peptide present a potentially useful approach to targeting atherosclerotic plaques.

While the CREKA micelles decorated the entire surface of plaques, the strongest accumulation of the micelles was at the shoulder, the junction between the plaque and the histologically healthy portion of the vessel wall, which are the sites most prone to rupture (Richardson, Davies et al. 1989). The high concentration of targeted micelles in the lesion shoulder suggests that these micelles may be effective in delivering compounds to rupture-prone plaques.

Increased fluorescence was observed in the aortic tree of atherosclerotic mice after injection of fluorescent CREKA micelles in imaging. We also examined the feasibility of imaging atherosclerotic plaques in intact animals. Unfortunately, CREKA micelles labeled with the infrared dye Cy7 did not produce a sufficient signal to visualize the plaques *in vivo* (data not shown), presumably because of insufficient tissue penetration of the exciting and emitted signals. The modularity of the micelles allows the construction of probes for more sensitive and penetrating imaging techniques, such as PET or MRI.

The homing of CREKA-coated iron-oxide nanoparticles to tumors is partially dependent on blood clotting induced by the particles within tumor vessels (2).



Importantly, CREKA micelles appear to be less thrombogenic than CREKA-coated iron oxide nanoparticles because the micelles, while homing to tumor vessels, did not induce any detectable additional clotting in them. Moreover, inhibiting blood clotting in atherosclerotic mice with heparin had no significant effect on the accumulation of CREKA micelles in the plaques. Thus, the thrombogenicity of CREKA micelles is low and they appear to target only preformed clotted material in both tumors and plaques.

Since the presence of the anticoagulant heparin did not significantly reduce CREKA micelle targeting to plaques and even longer term hirulog therapy did not reduce homing, we were able to use CREKA micelles to deliver an anticoagulant to these lesions. Like CREKA/FAM micelles, CREKA/hirulog mixed micelles accumulated in the rupture-prone shoulder regions of plaques and significantly increased anti-thrombin activity in the diseased vasculature. Thus, the CREKA micelle platform may be useful in reducing the clotting tendency in plaques and could potentially also reduce the risk of thrombus formation upon plaque rupture. Moreover, the targeting makes it possible to lower the dose, which should reduce the risk of bleeding complications.

### **Acknowledgements**

This chapter, in part, has been submitted for publication of the material as it may appear in *Proceedings of the National Academy of Sciences*, 2009, Targeting atherosclerosis using modular, multifunctional micelles. David Peters, Mark Kastantin, Ramana Kotamraju, Priya P. Karmali, Kunal Gujraty, Matthew Tirrell, and Erkki

Ruoslahti. The dissertation author was the primary investigator and author of this paper. We also thank Dr. Lilach Agemy for the 22RV1 mouse prostate tumor model and Peter Allen for the micelle graphic. This work was supported by National Heart, Lung and Blood Institute Program of Excellence in Nanotechnology Grant HL070818, and, in part, by NCCR Shared Instrumentation Grant 1S10RR017753 and MRSEC Program of the National Science Foundation Award DMR05-20415.

## References

- Alonso, A., A. Della Martina, M. Stroick, M. Fatar, M. Griebel, S. Pochon, M. Schneider, M. Hennerici, E. Allemann and S. Meairs (2007). "Molecular imaging of human thrombus with novel abciximab immunobubbles and ultrasound." *Stroke* **38**(5): 1508-14.
- Bode, C., M. Hudelmayer, P. Mehwald, S. Bauer, M. Freitag, E. von Hodenberg, J. B. Newell, W. Kubler, E. Haber and M. S. Runge (1994). "Fibrin-targeted recombinant hirudin inhibits fibrin deposition on experimental clots more efficiently than recombinant hirudin." *Circulation* **90**(4): 1956-63.
- Briley-Saebo, K. C., P. X. Shaw, W. J. Mulder, S. H. Choi, E. Vucic, J. G. Aguinaldo, J. L. Witztum, V. Fuster, S. Tsimikas and Z. A. Fayad (2008). "Targeted molecular probes for imaging atherosclerotic lesions with magnetic resonance using antibodies that recognize oxidation-specific epitopes." *Circulation* **117**(25): 3206-15.
- Davies, M. J. (1992). "Anatomic features in victims of sudden coronary death. Coronary artery pathology." *Circulation* **85**(1 Suppl): I19-24.
- Duguid, J. B. (1946). "Thrombosis as a Factor in the Pathogenesis of Coronary Atherosclerosis." *J Pathol Bacteriol* **58**(2): 207-212.
- Duguid, J. B. (1948). "Thrombosis as a factor in the pathogenesis of aortic atherosclerosis." *J Pathol Bacteriol* **60**(1): 57-61.
- Eitzman, D. T., R. J. Westrick, Z. Xu, J. Tyson and D. Ginsburg (2000). "Plasminogen activator inhibitor-1 deficiency protects against atherosclerosis progression in the mouse carotid artery." *Blood* **96**(13): 4212-5.

- Falk, E., S. M. Schwartz, Z. S. Galis and M. E. Rosenfeld (2007). "Putative murine models of plaque rupture." Arterioscler Thromb Vasc Biol **27**(4): 969-72.
- Ghigliotti, G., A. R. Waissbluth, C. Speidel, D. R. Abendschein and P. R. Eisenberg (1998). "Prolonged activation of prothrombin on the vascular wall after arterial injury." Arterioscler Thromb Vasc Biol **18**(2): 250-7.
- Houston, P., J. Goodman, A. Lewis, C. J. Campbell and M. Braddock (2001). "Homing markers for atherosclerosis: applications for drug delivery, gene delivery and vascular imaging." FEBS Lett **492**(1-2): 73-7.
- Ivey, M. E. and P. J. Little (2008). "Thrombin regulates vascular smooth muscle cell proteoglycan synthesis via PAR-1 and multiple downstream signalling pathways." Thromb Res.
- Karmali, P. P., V. R. Kotamraju, M. Kastantin, M. Black, D. Missirlis, M. Tirrell and E. Ruoslahti (2008). "Targeting of albumin-embedded paclitaxel nanoparticles to tumors." Nanomedicine.
- Kelly, K. A., M. Nahrendorf, A. M. Yu, F. Reynolds and R. Weissleder (2006). "In vivo phage display selection yields atherosclerotic plaque targeted peptides for imaging." Mol Imaging Biol **8**(4): 201-7.
- Liu, C., G. Bhattacharjee, W. Boisvert, R. Dilley and T. Edgington (2003). "In vivo interrogation of the molecular display of atherosclerotic lesion surfaces." Am J Pathol **163**(5): 1859-71.
- Maeda, N., L. Johnson, S. Kim, J. Hagaman, M. Friedman and R. Reddick (2007). "Anatomical differences and atherosclerosis in apolipoprotein E-deficient mice with 129/SvEv and C57BL/6 genetic backgrounds." Atherosclerosis **195**(1): 75-82.
- Maraganore, J. M., P. Bourdon, J. Jablonski, K. L. Ramachandran and J. W. Fenton, 2nd (1990). "Design and characterization of hirulogs: a novel class of bivalent peptide inhibitors of thrombin." Biochemistry **29**(30): 7095-101.
- Nakashima, Y., A. S. Plump, E. W. Raines, J. L. Breslow and R. Ross (1994). "ApoE-deficient mice develop lesions of all phases of atherosclerosis throughout the arterial tree." Arterioscler Thromb **14**(1): 133-40.
- Reddick, R. L., S. H. Zhang and N. Maeda (1994). "Atherosclerosis in mice lacking apo E. Evaluation of lesional development and progression." Arterioscler Thromb **14**(1): 141-7.

- Richardson, P. D., M. J. Davies and G. V. Born (1989). "Influence of plaque configuration and stress distribution on fissuring of coronary atherosclerotic plaques." Lancet **2**(8669): 941-4.
- Rosamond, W., K. Flegal, G. Friday, K. Furie, A. Go, K. Greenlund, N. Haase, M. Ho, V. Howard, B. Kissela, S. Kittner, D. Lloyd-Jones, M. McDermott, J. Meigs, C. Moy, G. Nichol, C. J. O'Donnell, V. Roger, J. Rumsfeld, P. Sorlie, J. Steinberger, T. Thom, S. Wasserthiel-Smoller and Y. Hong (2007). "Heart disease and stroke statistics--2007 update: a report from the American Heart Association Statistics Committee and Stroke Statistics Subcommittee." Circulation **115**(5): e69-171.
- Simberg, D., T. Duza, J. H. Park, M. Essler, J. Pilch, L. Zhang, A. M. Derfus, M. Yang, R. M. Hoffman, S. Bhatia, M. J. Sailor and E. Ruoslahti (2007). "Biomimetic amplification of nanoparticle homing to tumors." Proc Natl Acad Sci U S A **104**(3): 932-6.
- Smith, E. B. (1993). "Fibrinogen and atherosclerosis." Wien Klin Wochenschr **105**(15): 417-24.
- Stoll, P., N. Bassler, C. E. Hagemeyer, S. U. Eisenhardt, Y. C. Chen, R. Schmidt, M. Schwarz, I. Ahrens, Y. Katagiri, B. Pannen, C. Bode and K. Peter (2007). "Targeting ligand-induced binding sites on GPIIb/IIIa via single-chain antibody allows effective anticoagulation without bleeding time prolongation." Arterioscler Thromb Vasc Biol **27**(5): 1206-12.
- Whitman, S. C. (2004). "A practical approach to using mice in atherosclerosis research." Clin Biochem Rev **25**(1): 81-93.

## Chapter 5

### **Conclusion**

The goal of these experiments was to find new targeting elements that recognize atherosclerotic plaques, especially unstable plaques vulnerable to rupture, for delivery of diagnostic imaging agents and therapeutic drugs using nanoparticles. Being able to target unstable plaques using non-invasive techniques would advance the field of cardiology tremendously. As our understanding of the molecular mechanisms behind the destabilization of plaques advances it would be advantageous to have a means of delivering siRNA to the plaque to modify the expression of those genes involved. Also having the means to identify which plaques are vulnerable to rupture, which is not possible with current diagnostic modalities, would allow therapeutic intervention before an acute event occurs. The experiments in this paper identified a novel approach to targeting atherosclerotic plaques. By targeting the subtle clotting that occurs in the interior and on the surface of the plaques, those plaques that have ruptured can be identified and specific inhibition of coagulation and thrombus formation at the plaque could lead to fewer fatal acute events.

Various mouse models of atherosclerosis were studied to determine the feasibility of using these mice for *in vivo* phage screens to identify peptides that target vulnerable plaques. ApoE/SR-BI double knockout mice, which have advanced coronary atherosclerosis with many of the same features as the human disease including ECG abnormalities and myocardial infarction, were small, frail, and very difficult to

work with. The young age at which these mice began to show symptoms as well as the difficulty in isolating the diseased coronary vessels in the heart prevented *in vivo* phage display from successfully identifying new targeting peptides. Recently, alterations to the ApoE/SR-BI double knockout model have allowed the mice to survive longer. These mice might develop advanced lesions in the large vessels if they are allowed enough time for the disease to progress and would be easier to work since they are older. More experiments need to be done to determine if these alterations would make these mice more suitable for *in vivo* phage display.

ApoE knockout mice on a high fat diet were much easier to handle with large plaques in the main arteries. These mice are the most well studied animal model of atherosclerosis. Histology of the plaques demonstrated that the mice had stage V lesions after 6 months on the diet, which are very advanced plaques containing buried fibrous caps and other evidence of previous rupture. These mice were determined to be suitable for performing phage display to find targeting elements to vulnerable plaques but large numbers of mice are needed.

A potentially novel mouse model of plaque stabilization was created. Knocking out the R-Ras protein in the ApoE/SR-BI double knockout mouse had a significant effect on the lifespan of these mice. ApoE/SR-BI/R-Ras triple knockout mice lived for an average of 49 days compared to 43 days for the double knockout mice. More work needs to be done though to characterize the changes that occur in the plaques of these

mice and to determine if regulation of the expression of R-Ras could be used for stabilization of atherosclerotic plaques.

T7 phage were optimized for *in vivo* phage display by mutating the tail proteins. Four base pair substitutions in gene 17 caused conversion of two amino acids and changed the polarity of the residues, which disrupted the coiled-coil formation in the tail. Mutated phage remained infective in the circulation longer and were not cleared as quickly by the liver as wild-type T7 phage. By having more time to circulate, potential phage clones have an increased opportunity to bind to their target, potentially allowing each phage screen to be more effective. Additionally, previously impossible screens, due to high background in the liver, such as identifying peptides that bind to hepatocytes or the RES, may be possible with the mutated phage. Experiments to identify these peptides are ongoing in our lab. The positions of the tail mutations had previously been identified, but individual mutations allowed for a high reversion rate back to the wild-type phenotype, presumably due to the high mutation rate of phage. By inducing four base pair substitutions, the mutated phage were able to retain their altered phenotype even after 4 rounds of selection for liver binding. All of the phage that were sequenced even retained the complete mutated genotype.

*In vivo* phage display was performed in ApoE null mice on a high fat diet to determine if any of the peptides that had previously been identified in our lab to bind to tumor vasculature would also bind to atherosclerotic plaques. Atherosclerotic plaques have many similarities to the tumor microenvironment, such as hypoxia, inflammation,

angiogenesis, and oxidative stresses, therefore it was thought that some of the peptides might also bind the plaques. In a playoff screen using a pool of phage containing 10 different phage clones, phage that expressed CLT-1, CLT-2, and CREKA peptides were the most prevalent in the output of phage bound to the plaque. Phage were then individually tested for binding to atherosclerotic plaques *in vivo* and binding of the phage expressing the three peptides was substantially higher than binding of a control phage expressing glycine residues. All three peptides are known to target clotted plasma proteins, which are present in the stroma of tumors and in the interior and on the surface of atherosclerotic plaques.

Further T7 phage screens in ApoE knockout mice need to be performed. Most phage screens performed to identify targeting peptides for atherosclerotic plaques have used M13 filamentous phage that contain N-terminal fusion peptides on their surface. Presumably, since T7 phage express C-terminal fusion peptides, a different set of targeting peptides could be identified. Screens using randomized phage libraries for plaques vulnerable to rupture in ApoE knockout mice fed a high fat diet for extended periods of time could yield novel binding peptides that could give new insight into the process of destabilization.

Nanoparticles were targeted to atherosclerotic plaques in the ApoE knockout mouse on a high fat diet. We have developed multifunctional, modular micelles that contain a targeting element, a fluorophore and, when desired, a drug component in the same particle. These particles were targeted to atherosclerotic plaques with CREKA



peptide. The fluorescent micelles bound the entire surface of the plaque and notably, concentrated at the shoulders of the plaque, a location that is prone to rupture. The high concentration of micelles in the shoulder of the plaque suggests that these micelles might be effective at delivering compounds to plaques that are vulnerable to rupture.

Micelles coated with the CREKA peptide specifically targeted atherosclerotic lesions in ApoE null mice. The specificity of the targeting was evident from a number of observations: First, fluorescence from the micelles in the aortic tree of atherosclerotic mice localized to known areas of plaque formation and no fluorescence was observed in wild-type mice. Second, CREKA micelles bind to the entire surface of the plaque in histological sections, but do not bind to the healthy portion of the vessel. Third, an excess of unlabeled CREKA micelles inhibited the plaque binding of fluorescent CREKA micelles. Thus, CREKA targeted micelles present a potentially useful approach to targeting atherosclerotic plaques *in vivo*.

Fluorescence from CREKA targeted micelles was still observed in plaques even in the presence of heparin. This is important because CREKA iron oxide targeting was previously shown to be disrupted in the presence of heparin. This suggests that CREKA micelles target clotted plasma proteins that are already present on the plaque. Moreover, thrombogenicity of CREKA targeted micelles is low and unlike CREKA targeted iron oxide particles they do not induce clotting in either the diseased vessels of ApoE knockout mice or tumor blood vessels. Critically, CREKA micelles also retained their targeting ability after longer term anticoagulant therapy. Most patients in the hospital with unstable angina are on some form of anticoagulant therapy. CREKA

targeting even after 72 hours of intravenous thrombin inhibitor therapy means that CREKA-targeted micelles are good candidates for drug delivery to treat atherosclerosis.

CREKA targeted micelles are able to effectively deliver therapeutic drugs to the atherosclerotic lesions. The thrombin inhibitor peptide, hirulog, in CREKA/hirulog mixed micelles accumulated in the rupture-prone shoulder regions of plaques and significantly increased anti-thrombin activity in the diseased vasculature. Thus CREKA micelles are an effective platform for delivering both diagnostic imaging dyes and therapeutics to the atherosclerotic plaques.